Università degli Studi di Milano

GRADUATE SCHOOL OF VETERINARY SCIENCES
FOR ANIMAL HEALTH AND FOOD SAFETY
Director: Prof. Valentino Bontempo

Doctoral Program in Veterinary Clinical Sciences

Academic Year: 2012-2013

Appearance of ossification centers of the limbs and skeletal development in newborn toy-dog breeds: radiographic, morphometric and histological analysis

Melania Moioli

Tutor

Prof. Mauro Di Giancamillo

Coordinator

Prof. Fausto Cremonesi

Abstract

The study aims to find out the chronological appearance of the ossification centers of appendicular skeleton of newborn toy-breed dogs during the first month of life and to correlate the data obtained with morphometric measures of the skeleton by radiological and anatomical approach. Data obtained were implemented with bone mineral density (BMD) analysis of the long bones and histological and histochemical analysis of limbs bone sections, to evaluate and quantify the trends of the ossification process and the architectural changes of ossification centers.

The study was carried out in 37 newborn toy-breed dogs <28 days old, spontaneously died for unrelated reasons with this study, divided into 4 groups on the basis of age (first week, second week, third week and fourth week). The forelimbs and the hind limbs have been evaluated by radiological and histological analysis. Long bones, cranial and body measurements, both radiological and anatomical, were taken and the BMD of *radius* and *ulna* and of *os femoris* was calculated. The results have been correlated through statistical analysis and compared with standard charts proposed by Literature in order to assess significant differences with medium and large breed dogs.

The appearance of most of the ossification centers reflects the timing of ossification of medium and large breed dogs, however the behavior of some ossification centers changes and therefore might be considered typical of toy-dog breeds. Femoral length could be taken into consideration as a parameter to assess the developmental rate and the age of toy-breed dogs during the growing period, particularly in the first 4 weeks of age. Increasing BMD is highly correlated with increasing long bones length and seems to confirm the space-time relationship between BMD in canine newborn skeleton and in long bones growth.

The radiological, histological and bone mineral density analysis and the correlations between long-bones length, skull diameters, age and body mass, might be currently appropriate to determine the skeletal age in newborn toy-dog breeds.

Index

Introduction

Growth and weight gain within normal ranges is considered as part of the assessment of the overall health of young children and mammals. These processes are usually associated to dramatic changes in the bones and obviously of the whole skeletal conformation.

Bones in mammals develop via two distinct processes. Intramembranous bone formation produces many of the craniofacial bones directly from mesenchymal condensations (Percival and Richtsmeier, 2013). Conversely, endochondral ossification represents the principal process responsible for forming the most of the mammalian skeleton and generates bone via a cartilage intermediate (Mackie et al., 2011).

Endochondral bone growth progresses from proliferation, maturation and hypertrophy of chondrocytes, organized in ossification centers, to mineralization of cartilaginous matrix to form an osseous tissue. In long bones, endochondral bone growth and bone elongation are associated with calcium accretion mostly in the areas involved in architectural changes during the morphogenesis (Panattoni et al., 1999; Wongdee et al., 2012).

Estimation of age-at-death in skeletal remains has a long tradition in forensic science, because human skeleton undergoes sequential chronological changes. In human being there are numerous marker which can provide archaeologist and anthropologist with an estimate age of the deceased. The areas of skeletal remains that are commonly studied are cranial suture closure, dentition, epiphyseal closure, by means of radiographical analysis and bone microstructure. Recently, there has been increasing request for age estimation of living people undergoing criminal proceedings and in unaccompanied minor, when chronological age is not clear. Criteria that can be applied to investigate skeletons of children and adolescents are teeth mineralization status, length of longitudinal bones measurement and developmental status of the epiphysis (Cunha et al., 2009; Schmeling et al., 2007).

In living people, determination of the skeletal age of the left hand, through radiographic exam, plays a central role until final completion of maturation processes, at the age of approximately 18 years, even if age estimation is more relevant to first stages of life than in older children/adolescents because error range is lower in younger subjects (Cunha et al., 2009).

In this process, assessment of hand radiographs relies primarily on the stage of development of the epiphyseal ossification nuclei, the increase in size of the individual bones and of the hand skeleton as a whole, on changes in the shape of the various skeletal elements and on ossification of the epiphyseal plates (Schmidt et al., 2013b).

To date, dentition is the most widespread method for age estimation in growing dogs, even if literature, throughout the past years, has provided radiographic evaluation of the appearance and fusion of ossification centers in limbs bones, mainly concerning medium and large breed dogs (German Shepherd Dog (Charjan et al., 2002; Elmaz et al., 2008; Gustaffson et al., 1975; Hare, 1961), Greyhound (Gustaffson et al., 1975; Riser, 1975; Smith, 1960a, 1964; Smith, 1960b), Beagle (Chapman, 1965; Hare, 1961; Mahler and Havet, 1999; Yonamine et al., 1980)). Comparison with these studies is not simple due to not homogeneous data regarding especially the differences between large breed dogs and small breed toy dogs, considering that larger breeds have a longer growth period than smaller breeds (Hawthorne et al., 2004).

Recently, variation in the ossification processes of some long bones has been carried out in order to investigate abnormal skeletal development contributing to the development of skeletal pathologies (Breit et al., 2004; Mahler and Havet, 1999; Todhunter et al., 1997).

Skeleton of growing dogs has been also investigated with morphometric, radiographic photo-densitometric and bone mineral density studies (Delaquerriere-Richardson et al., 1982; Helmsmuller et al., 2013).

Morphometric analysis is usually employed during gestational age in order to establish the date of birth through ultrasound (Beccaglia et al., 2008b; Beccaglia and

Luvoni, 2012; Luvoni and Beccaglia, 2006), while some studies have been performed in order to establish breed standard by the measurements of the cranial diameters in German Shepherd Dog and in Cavalier King Charles Spaniel (Driver et al., 2010; Onar, 1999; Onar and Gunes, 2003; Schmidt et al., 2011), and to assess canine hip joint and stifle in large and giant breed dogs (Doskarova et al., 2010; Meomartino et al., 2002; Mostafa et al., 2009; Osmond et al., 2006).
Finally, single-photon absorptiometry and dual-energy X-ray absorptiometry (DEXA) have been employed to quantify long bone-healing in Boxer dogs (Zotti et al., 2004) and other breed dogs (Markel et al., 1990; Muir et al., 1995) and to determine the bone mineral density variations in different breeds (Markel et al., 1994), but not to correlate densitometric data with skeletal development and biological age. More recently, DEXA has been employed to study vertebral mineral density in German Shepherd dog to evaluate the resistance of the canine spine to traumatic lesions (Zotti et al., 2011).

Aim of the study

The dog is one of the most common companion animal: its growing processes and skeletal development are of major interest for breeders, owners and vets. Literature presents many papers regarding dog skeletal development in physiologic and pathologic conditions, but there are no sistematic papers regarding ossification centers appearance, allometry and bone mineral density in toy breed dogs.

Several papers have been published for the estimation of the age of growing dogs by evaluation of ossification centers, however data are not homogeneous and it is difficult to compare them. Most of these studies are focalized on medium and large breed dogs, moreover they evaluate subjects of different age and, finally, they analyze appearance and fusion of the centers with variable timing. Conversely, there

are very few indications concerning morphometry changes of the skeleton and of bone mineral density in growing dogs.

Aim of the study was to evaluate the chronological appearance of the ossification centers in the limbs of newborn toy-dog breeds during the first month of life and to correlate the data obtained with morphometric measures of the skeleton by a radiological and anatomical approach. Data obtained were implemented with bone mineral density analysis of the long bones and histological and histochemical analysis of limbs bone sections, to evaluate and quantify the trends of the ossification process and the architectural changes of ossification centers.

The choice to analyze the first month of life is related to the nature of the subjects analysed. Unlike previous studies in fact, which have been carried out on live animals or culled as part of the experimental design, for this study only animals died for reasons not related to the study were considered.

State of the Art

Endochondral ossification

Limb skeletal elements arise from the process of endochondral ossification, where cartilage serves as the initial anlage element and is later replaced by bone. This process is crucial in determining shape and size of definitive bones in vertebrates (Shimizu et al., 2007). Mouse genetic studies have provided several important insights about molecules regulating chondrocyte formation, chondrocyte maturation, and osteoblast differentiation, which are all key processes of endochondral bone development. These include the roles of the secreted proteins IHH, PTHrP, BMPs, WNTs, and FGFs, their receptors, and transcription factors such as SOX9, RUNX2, and OSX, in regulating chondrocyte and osteoblast biology (Long and Ornitz, 2013). Recent evidences suggest that ossification and rudiment

morphogenesis of limb bones, as well as other aspect of normal skeletogenesis, such tissue patterning during joint formation, require appropriate mechanical stimulation generated by embryonic movement (Nowlan et al., 2010), but very little is known about how the mechanical signals are integrated with classic biochemical signaling (Rolfe et al., 2013).

The cartilage model of a prospective bone develops as embryonic mesenchymal cells, which condense and differentiate into chondrocytes, and the chondrocytes secrete the various components of cartilage extracellular matrix (ECM). At the early stages of limb development the buds exhibit a paddle shape and consist of undifferentiated mesenchymal cells derived from the lateral plate and somatic mesoderm, covered by ectoderm (Shum et al., 2003).

The cartilage model expands through chondrocyte proliferation. Ossification of the cartilage model is preceded by hypertrophy of the chondrocytes in the prospective mid-shaft of the bone and by deposition of a periosteal bone collar by recently differentiated osteoblasts surrounding the mid-shaft. Blood vessels, osteoclasts (cartilage- and bone-resorbing cells), as well as bone marrow and osteoblast precursors then invade the model from the bone collar and proceed to form the primary center of ossification. The primary center expands towards the ends of the cartilage model, as the osteoclasts remove cartilage ECM and osteoblasts deposit bone on cartilage remnants. Generally, a secondary ossification center subsequently forms at each end of the cartilage model, leaving a cartilaginous growth plate between the primary and secondary ossification centers, as well as the prospective permanent articular cartilages at each end of the bone. The growth plate is responsible for longitudinal growth of bones.

Skeletal maturity occurs when the expanding primary center of ossification meets the secondary center of ossification, thus obliterating the growth plate.

Endochondral ossification starts during fetal life, and continues until the end of growth in early adulthood. Secondary ossification centers develop generally after birth. In dog some bones of the limbs develop entirely from one center of ossification. Other develop from two or more ossification centers, their appearance

and fusion occur in different time (Evans and Miller, 2013).

Ossification centers

(Hare, 1959b, 1960b, d, 1961; Ticer, 1984)

There are many papers reporting the ossification centers appearance and fusion in different breeds. On textbooks, the most reported data derive from Ticer (Ticer, 1984) (Tables 1 and 2).

Cingulum membri thoracici

Clavicula

Clavicula originates in the tendinous intersection of the brachiocephalicus muscle on day 28 of gestation and increases in size by the addition of bone formed in secondary cartilage. It continues to grow in size after birth as a thin plaque rather than as a hooklike nodule of earlier stages.

Scapula

Scapula develops from 2 principal ossification centers: one for the body (*corpus scapulae*) and one for the *tuber scapulae,* including coracoid process and *tuberculum supraglenoidale* (supraglenoid tuberosity). The first one derived from three ossification perichondral centers that, histologically, were identified at 35 days of gestation as a triangular area on the cranial margin of the *fossa supraspinata*, a short bar at the midpoint of the *spina scapulae*, and a plaque in the central area of the *fossa infraspinata*. They appear by day 40 and form a continuous perichondral collar around the *scapula*, although there is a distinct triangular region on the cranial edge of the *fossa supraspinata* that persists until birth.

Radiologically, at birth, the first ossification center is present and well developed, the second one develops later (Evans and Miller, 2013).

	Appearance	Fusion
SCAPULA		
Body	Birth	
Supraglenoid tuberosity (*tuberculum supraglenoidale*)	49	16-28
Coracoid process *(processus coracoideus*)		
HUMERUS		
Diaphysis	Birth	
Proximal epiphysis	7-14	40-52
Humeral condyles		to body at 24-32
Medial condyle	14-21	to lateral condyle at 24
Lateral condyle		
Medial epicondyle (*Epicondylus medialis*)	42-56	to condyles at 24
RADIUS		
Diaphysis	Birth	
Proximal epiphysis	21- 35	24-40
Distal epiphysis	14-28	32-48
ULNA		
Diaphysis	Birth	
Proximal epiphysis		
Olecranon	56	24-40
Distal epiphysis	56	32-48
CARPUS		
Ulnar carpal bone *(os carpi ulnare)*	28	
Radial *(os carpi radiale)*	21-28	
Central *(os carpi centrale)*	28-35	
Intermediate	21-28	
Intermedioradial carpal bone *(os carpi intermedioradiale)*		
Accessory carpal bone *(os carpi accessorium)*		
Body	14	
Epiphysis	49	16
First carpal bone *(os carpale I)*	21	
Second carpal bone *(os carpale II)*	28	
Third carpal bone *(os carpale III)*	28	
Fourth carpal bone *(os carpale IV)*	21	
Sesamoid bone	28	
METACARPUS		
Diaphysis	birth	
Distal epiphysis (2-5)*	28	24
Proximal epiphysis (1)*	35	24
PHALANGES		
First phalanx (Phalanx proximalis)		
Body (1-5)*	birth	
Distal epiphysis (2-5)*	28	24
Distal epiphysis (1)*	42	24
Second phalanx (Phalanx media)		
Body(2-5)*	birth	

Proximal epiphysis (2-5)*	35	24
Second phalanx absent or fused with first in first digit		
Third phalanx (Phalanx distalis)		
Body	birth	
Volar sesamoids	60	
Dorsal sesamoids	120	

Table 1 - Appearance (days) and fusion (weeks) of ossification centers of the forelimb in immature dog (Ticer "Radiographic technique in veterinary practice")

	Appearance	Fusion
HIP BONE (Os coxae)		
Pubis (*Os pubis*)	birth	16-24
Ilium (*Ilium*)	birth	16-24
Ischium (*Os ischii*)	birth	16-24
Acetabular bone (*Os acetabulum*)	49	20
Iliac crest (*Crista iliaca*)	120	1-2 years
Tuber ischii (*Tuber ischiadicum*)	90	32-40
Ischial arch (*Arcus ischiadicus*)	180	52
Caudal symphysis pubis	210	5 years
Symphysis pubis		5 years
FEMUR (*Os femoris*)		
Diaphysis	birth	
Proximal epiphysis (head)	14	28-44
Trochanter major	56	24-40
Trochanter minor	56	32-52
Distal epiphysis		to body 32-44
Femoral trochlea (Trochlea ossis femoris)	14	condyles to trochlea 12
Medial condyle (Condylus medialis)	21	
Lateral condyle (Condylus lateralis)	21	
PATELLA	56	
TIBIA (*Tibia*)		
Diaphysis	birth	
Condyles		to body 24-52
Medial condyle (Condylus medialis)	21	
Lateral condyle (Condylus lateralis)	21	
Tibial tuberosity (*Tuberositas tibiae*)	56	to condyles 24-48 to body 24-52
Distal epiphysis	21	32-44
Medial malleolus (*Malleolus medialis*)	90	20
FIBULA		
Diaphysis	birth	
Proximal epiphysis	56	32-52
Distal epiphysis	14-49	28-44
TARSAL BONES (*ossa tarsi*)		
Talus	birth-7	
Calcaneus	birth-7	
Tuber calcis	43	12024
Central tarsal bone (*Os tarsi centrale*)	21	
First tarsal bone (*Os tarsale I*)	28	
Second tarsal bone (*Os tarsale II*)	28	
Third tarsal bone (*Os tarsale III*)	21	
Fourth tarsal bone (*Os tarsale IV*)	14	
METATARSUS		

Metatarsus and pelvic limb phalanges are approximately the same as metacarpus and pectoral limb phalanges	
SESAMOIDS	
Fabellar	90
Poplitear	90
Plantar phalangeal	60
Dorsal phalangeal	150

Table 2 - Appearance (days) and fusion (weeks) of ossification centers of the hind limb in immature dog (Ticer "Radiographic technique in veterinary practice")

Skeleton brachii and antebrachii

The *humerus, radius* and *ulna* do not form epiphyses prior to birth.

Ossification of forefoot bones starts from 36 days of gestation, beginning from the metacarpals 2, 3, 4, and 5, which have perichondral ossifications at midshaft, the next ossifications occurred in the *phalanges distales*, followed by *phalanges proximales* and finally by *phalanges mediae*. *Digit II* and *digit III* are the first to ossify. Hind foot ossification follows the same order with slight variation. Although *ossa metacarpalia* and *phalanges* are ossified by the end of gestation, none of the *ossa carpi* ossify prior to birth (Evans and Miller, 2013).

Humerus

Most authors reported that *humerus* develops from 5 principals ossification centers: one for the body, one for the proximal epiphysis (formed by *caput humeri* (head), *tuberculum majus* (greater tubercle) and *tuberculum minus* (lesser tubercle)), 2 for the *condilus humeri* (humeral condyle) in the distal epiphysis (one for the *capitulum* and one for *trochlea* respectively), and finally one for the *epycondylus medialis* (medial epicondyle).

Radius

All the Authors indicate that *radius* develops from 3 principal ossification centers, one for the *corpus radii* (body), one for the *caput radii* (head) in the proximal epiphysis and one for the *trochlea radii* (trochlea) in the distal epiphysis.

Ulna

Ulna develops from 3 principal ossification centers, one for *olecranon* and the *corpus ulnae* (body), one for the *tuber olecrani* (olecranon tuberosity) and one for the *caput ulnae* (head of the ulna), in the distal part of the bone. Few Authors described a further ossification center for the anconeal process in different breeds and in the Beagle Dog (Chapman, 1965; Hare, 1959b). Recently, the presence of this center has been investigated in large breed dogs because its presence can be related to elbow dysplasia (Breit et al., 2004; Cook and Cook, 2009; Cross and Chambers, 1997; Frazho et al., 2010; Gasch et al., 2012; Michelsen, 2013), but its presence in toy breed dogs has not been definitely demonstrated.

Skeleton manus

The *skeleton manus* is composed by *ossa carpi, ossa metacarpalia I-V* and *ossa digitorum manus.*

Ossa carpi

The *ossa carpi* (carpal bones) are arranged in a proximal and a distal row. The bones of the proximal row are *os carpi intermedioradiale* (intermedioradial carpal bone), *os carpi ulnare* (ulnar carpal bone) and *os carpi accessorium* (accessory carpal bone). The bones of the distal row are *os carpale I* (first carpal bone), *os carpale II* (second carpal bone), *os carpale III* (third carpal bone) and *os carpale IV* (fourth carpal bone).

Hare reported that *carpus* develops from 10 ossification centers. There is just one center for the ulnar carpal bone, the first carpal bone, the second carpal bone, the third carpal bone and the fourth carpal bone.

The accessory carpal bone is formed by two centers, one for the basal enlarged surface (body of the accessory bone) and one for the free end or epiphysis.

The intermedioradial carpal bone *(os carpi intermedioradiale)* represents the fusion of 3 ossification centers: *os carpi radiale*, *os carpi intermedium* and *os carpi centrale.*

As showed in table 1-2, the age and, although slightly, the chronological order of appearance at which the carpal centers of ossification appears differs between breeds. However, it is generally indicated that the center for the body of the accessory bone is the first that appears, and successively the centers for the other carpal bones appear and finally the epiphysis of the accessory bone that elaborates the cap of the enlarged palmar end of the bone.

Ossa metacarpalia and *ossa digitorum manus*

Ossa metacarpalia and *ossa digitorum manus* will be explained at the end of the chapter together with *ossa metatarsalia* and *ossa digitorum pedis*.

Cingulum membri pelvini

The pelvic girdle is completely cartilaginous until gestational day 40, when a perichondral bone collar develops around *os ilium*. Several days later (day 45) *os ischii* ossifies and appears shortly before or at birth (day 55 to 60). *Os pubis* appear until several weeks after birth (Evans and Miller, 2013).

The *cingulum membri pelvini* develops from 8 centers of ossification: one for the body (*corpus ossis ilii)* and the wing *(ala ossis ilii)* of *os ilium*, one for the body *(corpus ossis ischii)* and the *ramus (ramus ossis ischii*), of *os ischii*; one for the body *(corpus ossis pubis)* and the *ramus (ramus ossis pubis*) of *os pubis*; one for the acetabular bone *(os acetabulum),* one for the iliac crest *(crista iliaca)* and one for the ischiatic tuberosity *(tuber ischiadicum)*. The ischial arch *(arcus ischiadicus)* develops from one or more ossification centers. Moreover there is a small center for the interischiaticum bone, a small bone, wedge shaped, which develops in the angle of divergence between *os ischii* and the caudal end of the pelvic symphysis.

Skeleton femoris and cruris

Os femoris, tibia and *fibula* ossify first perichondrally as *ossa metatarsalia* and *phalanges* do. A cartilaginous *patella* is present in the tendon of the *musculus quadriceps femoris* throughout the second half of gestation. Only *talus* and *calcaneus* ossify before birth in *ossa tarsi.*

Os femoris

Os femoris (femur) develops from 5 center of ossification, one for the *corpus ossis femoris* (body), one for the *caput ossis femoris* (head), one for the *trochanter major* (greater trochanter), one for the *trochanter minor* (lesser trochanter) in the proximal epiphysis and one for the *condylus lateralis* (lateral condyle) and the *condylus medialis* (medial condyle) in the distal epiphysis. Moreover, few Authors reported even a sixth ossification center in the distal epiphysis for the *trochlea ossis femoris* (femoral trochlea)(Ticer, 1984; Zoetis et al., 2003).

Tibia

Tibia develops from 5 centers of ossification one for the *corpus tibiae* (body), one for the *condylus lateralis* and *medialis* (lateral and medial condyles), one for the *tuberositas tibiae* (tibial tuberosity), one for the *malleolus medialis* (medial malleolus) and one for the *cochlea tibiae* (distal epiphysis).

Fibula

Fibula develops from 3 centers of ossification: one for the *caput fibulae* (head of the fibula), one for the *corpus fibulae* (body of the fibula) and one for *malleolus lateralis* (lateral malleolus).

Skeleton pedis

The skeleton pedis is composed by *ossa tarsalia, ossa metatarsalia I-V* and *ossa digitorum pedis.*

Ossa tarsalia

Calcaneus and *talus* make up the proximal row of the *ossa tarsalia* (tarsal bones), while the distal row consists of four bones. Three small bones, *os tarsale I, II, III* (first, second and third tarsal bones), separated from the proximal row by the *os tarsi centrale* (central tarsal bone). Finally, *os tarsale IV* (fourth tarsal bone) completes, laterally, the distal row.

Each bone develops from a single ossification center, except *calcaneus*, which develops from two different centers, one for body and the processus of calcaneus and one for the proximal half of the bone (*tuber calcanei*). The centers for the body and the processus of *calcaneus* and *talus* appear before birth, the remaining centers appear after birth.

Ossa metacarpalia and *metatarsalia*

Ossa metacarpalia and *metatarsalia II* to *V* (metacarpal and metatarsal bones II to V) are the best developed. Each of them develops from 2 ossification centers, one for the *caput* (head) and one for the distal epiphysis and the body. The center for the body is well developed at birth, while the center for the head appears in different time: the center in the 3rd and 4th bones appears first, the center for the 2nd bone appears after the first two and the center of the 5th bone develops later. The centers for the head in the metacarpal bones appear slightly later than those in the metatarsal bones.

The metarcarpal bone I develops from 2 ossification centers, but, in this case, one is for the diaphysis and the other one is for the proximal epiphysis.

Metatarsal bone I varies between individual and breeds. Usually it derives from a single ossification center, which appears in different time.

Phalanges (ossa digitorum manus and *pedis)*

The first or proximal phalanx *(phalanx proximalis*) and the second or middle phalanx *(phalanx media)* develop from 2 centers of ossification, one for the *corpus* (body) in middle position and the *caput* (head) in the distal position, and one for the *basis*, in proximal position.

The *basis* in the forelimb appears before the one in the pelvic limb and the *basis* in the axial digits before those of the abaxial digits.

The distal phalanx of each digit develops from a single center of ossification, which is present at birth.

Ossa sesamoidea

Each *os sesamoideum* (sesamoid bone) develops from a single center of ossification, both in pectoral and in pelvic limb in different time (table 1-2). The first to appear are located on the palmar/plantar surface of each metacarpophalangeal joint or metatarsophalangeal joint.

In forensic anthropology, age estimation both on the dead and the living needs still updating and organization. Uniforming methods and procedures is basic both for the dead and the living, in fact, aging the dead means to create a biological profile that can be compared to missing persons, while aging the living, especially children and minors, helps in solving judicial or civil problems (Cunha et al., 2009; Schmeling et al., 2007).

Several reviews on aging have been carried out in the past (Cunha et al., 2009; Franklin, 2010; Schmeling et al., 2007) and they said that different methods are more or less suitable for aging people of different age and for aging cadavers, remains and body parts. There are no methods unanimously accepted because most methods suffer from sex and ethnic bias and, regarding aging the dead, even from the preservation of bodies or remains. Moreover for most of the methods, a standard error in age estimation goes from 6 months to 2 years or more and it is neither homogeneous because a lower error occurs in younger subjects, while age estimation in adults is more difficult because skeletal and dental development have already advanced (Cunha et al., 2009).

For these reasons, before applying a method, it method must be presented to the scientific community by publication in peer-reviewed journals and have demonstrated accuracy (Cunha et al., 2009; Schmeling et al., 2007). Information about the accuracy of age estimation must be clearly available and in aging the living, principles of ethical and medico-legal regulations must to be considered (Cunha et al., 2009; Schmeling et al., 2007). The study of dental development and the measurements of long bones diaphyseal length represent some methods for aging dead newborns, infants and children, while the evaluation of the presence of ossification nuclei, of the mineralization of cuspid of first permanent molar and of the ossification of the femoral distal epiphysis are useful only in aging dead newborn. Maturation of hand and wrist, fusion of the sternal end of the clavicle and hormonal variations are some of the methods employed to age subadults, while

the observation of physiological degeneration of skeletal and dental structures, the evaluation of *os coxae*, ribs and cranial sutures are more suitable for aging adults (Boyne et al., 2010; Cunha et al., 2009; Franklin, 2010). The analysis of osteons, the carbon-14 analysis, the study of periodontal diseases and DXA bone densitometry are only few examples of the methods used for aging cadavers, remains and body parts (Castillo and Ruiz Mdel, 2011; Cunha et al., 2009).

Aging the living starts from a physical examination and a collection of medical information through a complete patient history (which in adults can be completed by clinical tests). In children and young adults skeletal and dental evaluation are the most used methods, while there are only a few methods that can be employed in aging adults, like a general evaluation of physical status (with hormonal dosage for women) and the amino acid racemization on dentine (Cunha et al., 2009).

A radiological examination is often used in forensic anthropology in aging both the dead and the living (Cunha et al., 2009). The radiologists look for the ossification centers, for their appearance and their fusion and compare the findings with an atlas (Cunha et al., 2009; Greulich and Idell Pyle, 1975; Schmidt et al., 2013a).

Unfortunately, often there isn't a perfect match between biological and chronological age because the growth differs in different ethnic groups and in different ages, and it could be influenced by nutritional and individual factors (Cunha et al., 2009). Therefore, literature often refers to populations who are different from those under examination and the individual biological variability must be added to these problems. There are no uniformity of procedures and methods employed and it would be valued "if minimum image quality requirements were to be drawn up for the various radiographic procedures" (Schmeling et al., 2007).

Another method used in forensic anthropology in aging both dead and living newborns, infants and children is the measurement of diaphyseal length of long bones (Cunha et al., 2009; Franklin, 2010). Furthermore, the most common methods employed to estimate subadult age-at-death are based both on metrical

and morphological analysis of ossification centers, while new approaches tend to quantify even size and shape variation of ossification centers (Franklin, 2010).
Other Authors reported also that Dual-energy X-ray Absorptiometry (DXA) could be employed to investigate the appearance of ossification centers on specimens and that "it is a more reliable technique for spatial resolution, precision and accuracy" (Panattoni et al., 2000; Panattoni et al., 1999).

Skeletal evaluation and age determination in Veterinary Medicine

In Veterinary Medicine, it's even more difficult because there are more breeds, often affected by different growth and skeletal pathologies (Boulay, 1998; Doskarova et al., 2010; Fries and Remedios, 1995; Fujiki et al., 2007; Gasch et al., 2012; Smolders et al., 2013). For these reasons every method employed to estimate the biological age of a young dog might consider the breed variability.
Growth and skeletal development, as in human being, are also influenced by nutritional and individual factors (Vanden Berg-Foels et al., 2006) and the rapid growth is a further difficulty in Veterinary Medicine because dogs become adults in a shorter time.
There are many papers concerning the appearance of ossification centers in dog but often they are not homogeneous for the methods and the breeds employed, the ages and the anatomical compartments investigated, and for the reason of the investigation (such as skeletal pathologies or delayed ossification). Moreover, some studies have been carried out only to compare maturation processes of ossification centers in different species and not only in dog (Fukuda and Matsuoka, 1980; Kilborn et al., 2002; Zoetis et al., 2003).
The first paper dealing with the study of mammalian ossification centers through dissection and maceration goes back to the 1884 (Lesbre, 1897; Retterer, 1884), while the first radiologic papers go back to the 1948 (Seoudi, 1948). Most of the papers have been published in the 60's (Bressou et al., 1957; Chapman, 1965; Hare, 1959a, b, 1960a, c, d, 1961; Pomriaskinsky- Kobozieff and Kobozieff, 1954; Smith,

1960a,b; Sumner-Smith, 1966), while in 1978 Schebitz (Schebitz and Wilkens, 1978) showed one of the most complete table dating appearance and fusion of ossification centers of forelimb and hind limb in German Shepherd Dog. However neither the breeds or the number of dogs enrolled or the interval of examinations were reported, these papers are still cited and used to establish the age of growing dogs because from the 70's Authors focused their attention only on ossification centers of the long limb bones and on the pelvis and they correlate the ossification process to the development of growing pathologies (Breit et al., 2004; Frazho et al., 2010; Fukuda and Matsuoka, 1980; Kilborn et al., 2002; Madsen et al., 1991; Mahler and Havet, 1999; Riser, 1973, 1975; Todhunter et al., 1997; Vanden Berg-Foels et al., 2011; Zoetis et al., 2003). More recently, Authors focused their attention even on the nutritional factors that can affect skeletal development and growing pathologies (Hedhammar et al., 1974a; Hedhammar et al., 1974b; Vanden Berg-Foels et al., 2006; Wu et al., 1974)

Finally, results of some of the previous papers have been collected and reported in some textbooks ("Veterinary Radiology" (Carlson, 1967), "Textbook of Small Animal Orthopaedics" (Newton, 1985), "Textbook of veterinary anatomy" (Dyce et al., 2010), "Radiographic Technique in Veterinary practice"(Ticer, 1984), "Diagnostic Radiology of the dog and the cat"(Kealy, 1987), "Small Animal Radiology and Ultrasound: A Diagnostic Atlas and Text" (Burk and Feeney, 1996), "Handbook of small animal radiology and ultrasound Techniques and differential diagnoses" (Dennis et al., 2010)), even if number of dogs nor breeds enrolled nor the interval of examinations were always reported.

Another method used to evaluate skeletal development in growing subjects is represented by morphometric analysis. Anatomical morphometry and radiological morphometry are different branches of the same discipline and they are used to measure different anatomical parts, repeatedly, in order to correlate them between different subjects or breeds and with different parameters.

There are many papers concerning this topic, especially regarding morphometric analysis applied to diagnostic imaging, in order to establish the gestational age of

the *fetus*, both in Human and in Veterinary Medicine (Garmel and D'Alton, 1994; Kutzler et al., 2003; Lopate, 2008). Recently, MRI has been proposed as a method to evaluate the ossification process and to correlate it with the gestational age of the *fetus* and with the development of skeletal pathologies, both in Human and in Veterinary Medicine (Connolly et al., 2004; Nemec et al., 2013). In dog, most of the morphometric studies have been carried out to measure cranial diameters in order to establish breed parameters, both in fetuses and in adult dogs (Evans and Miller, 2013; Onar, 1999; Onar and Gunes, 2003; Schmidt et al., 2011). Recently, radiological morphometry has been employed to evaluate canine hip joint (Doskarova et al., 2010; Meomartino et al., 2002) and skeletal characteristics of pelvic limbs in dogs with and without cranial cruciate ligament rupture (Mostafa et al., 2009; Osmond et al., 2006) or with and without patellar luxation (Mostafa et al., 2008).

There are only a few papers regarding morphometry and skeletal development in dogs and both studies have been carried out on Beagle dogs (Delaquerriere-Richardson et al., 1982; Helmsmuller et al., 2013). In the first study they performed a correlation between age, body weight, x-ray morphometrical measurements and x-ray photodensitometry of the bones of standardized colony-raised male research Beagles of 13 and 21 months (Delaquerriere-Richardson et al., 1982); while the second study is a quite extended paper regarding the ontogenetic allometry of the Beagle. They monitored the ontogenetic development of 6 Beagle between 9 and 51 weeks of age to investigate their skeletal allometry and compare these results with data from others lines, breeds and species (Helmsmuller et al., 2013).

To our knowledge, there are no papers regarding the employment of Dual-energy X-ray Absorptiometry (DXA) to investigate the appearance of ossification centers in Veterinary Medicine, but single-photon absorptiometry and dual-energy X-ray absorptiometry (DEXA) have been employed to quantify long bone-healing (Markel et al., 1990; Muir et al., 1995; Zotti et al., 2004), to determine bone mineral density variations in different breeds (Markel et al., 1994), to evaluate the

relationship between the "moment of resistance" of the canine spine (Zotti et al., 2011) and to investigate other pathological conditions (Burton et al., 2010; Emmerson et al., 2000; Isola et al., 2005).

Materials and methods

37 newborn toy-dog breeds <28 days old, (body weight < 7kg (Brianza et al., 2006), 19 females and 18 males), spontaneously died for unrelated reasons with this study were enrolled. They derived from the local veterinary clinics and they were supplied with the consent of the owners. They were collected and immediately frozen, and later they were subjected to radiographic examination, densitometry and histological sampling. Based on the age of the subjects, they were divided into 4 groups: group 1 (till 7 days of age), group 2 (8 to 14 days of age), group 3 (15 to 21 days of age) and group 4 (from 22 to 28 days of age). For each cadavers, body weight was recorded.

Radiographic analysis

Radiographic studies were performed through two CR systems (Agfa ADC COMPACT® e FCR Fuji Capsula X) assembled with a radiological unit (ARCOM - Simply) with double focal spot (0,6 and 1,3 mm), 32 kW of nominal anode input power and inherent filtration of 0,7 mm Al eq. The focal spot-film distance was 100 cm and the central ray was perpendicular to the film in all the radiographs. When the position of the carcasses was not ideal, a wider acquisition field compared to the district investigated was employed. For every dog different radiographic projection were performed: latero-lateral (LL) and dorso-ventral (DV) of the head, medio-lateral (ML) and cranio-caudal (Cr-Cd) of the forelimb, medio-lateral (ML) and caudo-cranial (Cd-Cr) of the hindlimb and latero-lateral (LL) and dorso-ventral (DV) of the whole body.

Latero-lateral views of the head and of the whole body were obtained placing the dogs on left lateral recumbency with the forelimbs and the hind limbs superimposed and fixing them at the radiographic cassettes with radiolucent adhesive tape. The head were placed in lateral position through radiolucent devices and fixed at the radiographic cassettes with radiolucent adhesive tape. Dorso-

ventral views were performed placing the dogs *on ventral recumbency* and the flexed arms externally in contact with the radiographic cassettes and fixing them with radiolucent adhesive tape.

Medio-lateral views of the forelimb were obtained by placing the dogs on the side of the radiographed limb. The contralateral limb was carefully moved caudally, superimposed with the body and fixed with radiolucent adhesive tape. Cranio-caudal views were obtained placing the dogs *on ventral recumbency*, extending the radiographed forelimb cranially and fixing it at the radiographic cassettes with radiolucent adhesive tape.

Medio-lateral views of the hindlimb were obtained by placing the dogs on the side of the radiographed limb. The contralateral limb was carefully moved cranially, superimposed with the body and fixed with radiolucent adhesive tape. Caudo-cranial views were performed placing the dogs *on ventral recumbency,* extending the radiographed hindlimb caudally and fixing it at the radiographic cassettes with radiolucent adhesive tape.

All images were storage in an Apple data base and post processing evaluation and measurement were performed by OsiriXPRO software (Apple ®).

Ossification centers

The standard for evaluation of an ossification center was the appearance of a radiopaque area on radiograph at the level of the corresponding bone (Hare, 1959b).

The centers taken into consideration were the following:

-forelimb: proximal and distal epiphysis of *humerus, radius* and *ulna*, *ossa carpi*;

-hindlimb: *os ischii, os ilium* and *os pubis*, proximal and distal epiphysis of *os femoris, tibia* and *fibula*; *patella* and *ossa tarsi* (Authors Committee, 2012).

Long bones measurements

Long bones measurements of humeral, radial and ulnar lengths of the left forelimbs and of femoral and tibial lengths of the left hindlimbs were measured on the medio-lateral projections. At birth it's difficult to measure the lengths of long bones because only the diaphysis are radiopaque, therefore for newborn dogs the long bones lengths correspond with the lengths of the diaphysis (Riser, 1973).

Craniometric and body length measurements

The skull, the cranial and the viscero-cranial lengths, the neurocranium and the zygomatic widths were measured on the dorso-ventral projections of the head. The skull length (SL) was measured from the external occipital protuberance to the anterior end of the interincisive suture. The cranial length (CL) from the junction on the median plane of the right and left nasofrontal sutures to the external occipital protuberance. The viscero-cranial length (VL) from the junction on the median plane of the right and left nasofrontal sutures to the anterior end of the interincisive suture. The neurocranium width (NW) from the most lateral point of the brain case to the one of the other side. The zygomatic width (ZW) was measured from the most lateral point of one zygomatic arch to the most lateral point of the other (Onar, 1999; Schmidt et al., 2011). Crown-rump and vertebral column lengths were measured on the latero-lateral projections of the whole body (Evans and Miller, 2013). Crown-rump length (CRL) was measured from the junction on the median plane of the right and left nasofrontal sutures to the *anum*. Vertebral column length (VCL) was measured from the first cervical vertebra to the end of the tail (Evans and Miller, 2013).

In order to reduce the inaccuracies, each measurement was taken three times by a single operator.

Densitometric analysis

Bone mineral density (BMD) was calculated on a minimum of two samples for each group without the skeletonization of the limbs: 5 specimens of group 1, 4 specimens of group 2, 3 specimens of group 3, 2 specimens of group 4.
The specimens were scanned by means of a DEXA device (Hologic QDR-1000, Hologic, Waltham, MA, USA). Each specimen was scanned standing horizontally, with a disto-proximal direction and in a medio-lateral projection. Before scanning the unit was always calibrated by means of own calibration phantom (Hologic Calibration Phantom, Hologic). The general BMD of *radius* and *ulna* and of *os femoris* were calculated. The BMD results were expressed as grams of bone mineral on the scanned site area (g/cm2) (Panattoni et al., 1999; Zotti et al., 2011). Each scan was performed by the same operator.

Anatomical and histological analysis

Anatomical and histological analysis were performed on the same animals selected for densitometric analysis.

Histological analysis
After skeletonization of the limbs, samples were fixed in buffered 10 % formalin (Bio-Optica, Milan, Italy) and further decalcified with 45% formic acid (Sigma Chemical Company, St. Louis, USA), for 2-3 days and successively with 15% 0.5 M EDTA solution (Sigma Chemical Company, St. Louis, USA) (pH 8.0) for 7 days as indicated by Ozaki et al with a slight modification (Ozaki et al., 2010). Subsequently, they were dehydrated in graded alcohol and xylene series and embedded in paraffin. Serial sections (4µm) were mounted on the glass slides previously treated with Vectabond (Vector Laboratories, Burlingame, CA, USA) to enhance the adherence of tissue. Sections were stained with ematoxilin-eosin and Thichrome Staining (Masson- Bio-Optica.).

Proximal and distal epiphysis of *humerus*, proximal and distal epiphysis of *radius* and *ulna* and *ossa carpi*, proximal and distal epiphysis of *os femoris*, proximal and distal epiphysis of *tibia* and *ossa tarsi* were examined.

Long bones measurements

Humeral, radial, femoral and tibial lengths were measured using a caliber before the skeletonization of the limbs. Measures were acquired on the lateral sides of each left limbs. The humeral length was measured from the most distal point of the *trochlea* to the most proximal point of the *caput humeri*, the radial length was measured between the most proximal and distal points of the bone, the femoral length was measured between the most proximal and distal points of the bone and the tibial length was measured between the most proximal and distal points of the bone (Alpak et al., 2004).

Craniometric and body length measurements

Skull length, neurocranium width, (Alpak et al., 2004) crown-rump and vertebral column lengths (Evans and Miller, 2013) were measured using a caliber and/or a ruler without skeletonization of the cadavers.

In order to reduce the inaccuracies, each measurement was taken three times by a single operator

Statistical analysis

Statistical analyses were performed with the IBM SPSS Statistics 21.0 (IBM SPSS Inc., Armonk, USA).

Before any statistical test, data distribution was verified by the mean of Shapiro-Wilk test. Radiographic and anatomical measurements were compared with Friedman's test to investigate the repeatability of their mean values.

Pearson's correlation coefficient was employed to correlate the radiographic measures with body mass and days of age and to correlate the anatomical measures with body mass and days of age.

A non parametric Sperman bivariate correlation was employed to perform the correlation between radiographic and anatomical measures for each measurement. Sperman bivariate correlation was employed to match the different bone mineral densities calculated respectively in the forelimb and in the hindlimb with the radial and ulnar lengths, and with the femoral length.

U-Mann-Whitney test was employed to match the appearance on the radiographs of *caput humeri* with humeral length, the appearance on the radiographs of *os pubis* with femoral length and the appearance on the radiographs of *calcaneus* and *talus* with femoral and tibial lengths. ANOVA test was employed to match the appearance of *corpus ossis accessorii* with radial and ulnar lengths, the appearance of *caput ossis femoris* with femoral length and to match the appearance of *os tarsale IV* with the tibial length.

Results

The sample size was composed of 37 new-born toy-dog breeds <28 days old, (body mass < 7kg (Brianza et al., 2006), 19 females and 18 males). The breeds resulted Chihuahua, Maltese, Toy Poodle, Shi-Tzu (4 dogs), Miniature Pinscher (2 dogs) and Jack Russel Terrier (3 dogs) and the most representative breeds resulted Chihuahua (13 dogs), Maltese (8 dogs) and Toy Poodle (7 dogs) (table 3).

Group 1 (till 7 days of age) was composed of 25 subjects, group 2 (8 to 14 days of age) was composed of 7 subjects, group 3 (15 to 21 days of age) was composed of 3 subjects and group 4 (from 22 to 28 days of age) was composed of 2 subjects (table 3).

The mean body mass was 118,78 g in group 1, 114,71 g in group 2, 161,66 g in group 3, 265 g in group 4.

Number	Group	Age (days)	Sex	Weight (g)	Breed
1	1	1	M	185	Chihuahua
2	1	1	M	97	Chihuahua
3	1	1	F	100	Maltese
4	1	1	M	121	Chihuahua
5	1	1	M	60	Chihuahua
6	1	1	F	100	Maltese
7	1	1	F	80	Miniature Pinscher
8	1	1	F	130	Chihuahua
9	1	1	M	160	Chihuahua
10	1	1	F	250	Jack Russel Terrier
11	1	1	F	162	Chihuahua
12	1	1	M	71	Chihuahua
13	1	1	M	152	Jack Russel Terrier
14	1	1	F	81,6	Jack Russel Terrier
15	1	2	M	100	Toy Poodle
16	1	2	M	96	Toy Poodle
17	1	3	M	95	Chihuahua
18	1	3	F	90	Toy Poodle
19	1	3	F	90	Toy Poodle
20	1	5	F	165	Toy Poodle
21	1	5	F	83	Maltese
22	1	5	M	95	Shi-Tzu
23	1	5	M	131	Shi-Tzu
24	1	7	F	125	Chihuahua
25	1	7	M	150	Shi-Tzu
26	2	8	F	61	Toy Poodle
27	2	8	M	71	Toy Poodle
28	2	10	F	60	Miniature Pinscher
29	2	10	F	255	Maltese
30	2	10	F	111	Maltese
31	2	12	F	130	Maltese
32	2	13	F	115	Chihuahua
33	3	15	M	165	Maltese
34	3	15	M	135	Maltese
35	3	21	F	185	Shi-tzu
36	4	25	M	250	Chihuahua
37	4	28	M	280	Chihuahua

Table 3 - Sample size, group, age, sex, body mass, breed

Radiographic analysis

Evaluation of ossification centers

All the diaphysis of the limbs were present in all the subjects of the four groups (37/37) (fig. 1-2) and no differences between right and left limbs were recorded.

Figure 1 - Medio-lateral projection of the right forelimb of a 21-days-old Shi-Tzu.

Figure 2 - Medio-lateral projection of the right hind limb of a 21-days-old Shi-Tzu.

All the diaphysis are evident, in the forelimb *clavicula* and ossification centers of *caput humeri* are evident, while in the hind limb *os pubis, calcaneus* and *talus* are evident.

Humeral proximal epiphysis appeared in 0/25 subjects of group 1, in 3/7 subjects of group 2, in 3/3 subjects of group 3, in 2/2 subjects of group 4; *trochlea humeri* appeared in 0/25 subjects of group 1, in 1/7 subjects of group 2, in 1/3 subjects of group 3, in 2/2 subjects of group 4 (fig. 3); *capitulum humeri* appeared in 0/25 subjects of group 1, in 1/7 subjects of group 2, in 1/3 subjects of group 3, in 0/2 subjects of group 4 and *epicondylus medialis* appeared in 0/25 subjects of group 1, in 1/7 subjects of group 2, in 0/7 subjects of group 3, in 0/2 subjects of group 4.

Figure 3 - Medio-lateral projection of right *humerus* of a 28-days-old Chihuahua. The ossification centers of *caput humeri, trochlea humeri* and *caput radii* are evident.

Caput radii appeared in 0/25 subjects of group 1, in 0/7 subjects of group 2, in 0/3 subjects of group 3, in ½ subjects of group 4 (fig. 3) and *trochlea radii* appeared in 0/25 subjects of group 1, in 0/7 subjects of group 2, in 0/3 subjects of group 3, in 2/2 subjects of group 4.

Tuber olecrani and *caput ulnae* did not appear in any subjects analyzed.

Os carpi radiale appeared in 0/25 subjects of group 1, in 0/7 subjects of group 2, in 0/3 subjects of group 3, in ½ subjects of group 4; *os carpi intermedium* appeared in 0/25 subjects of group 1, in 0/7 subjects of group 2, in 0/3 subjects of group 3, in 2/2 subjects of group 4; *os carpi centrale* appeared in 0/25 subjects of group 1, in 0/7 subjects of group 2, in 0/3 subjects of group 3, in 0/2 subjects of group 4; *os carpi ulnare* appeared in 0/25 subjects of group 1, in 0/7 subjects of group 2, in 0/3 subjects of group 3, in 2/2 subjects of group 4. *Os carpi accessorium* appeared in 0/25 subjects of group 1, in 2/7subjects of group 2, in 1/3 subjects of group 3, in 2/2 subjects of group 4 and *ossa carpi I, II, III, IV* appeared in 0/25 subjects of group 1, in 1/7 subjects of group 2, in 0/3 subjects of group 3, in ½ subjects of group 4 (fig. 4) (table 4).

Figure 4 – Cranio-caudal projection of right *carpus* of a 28-days-old Chihuahua. The ossification centers of *trochlea radii, os carpi radiale, os carpi intermedium, os carpi ulnare,* the body of *os carpi accessorium*, *ossa carpi I, II, III, IV* are evident.

Os ischii was present in all the subjects of the four groups (37/37).

Os pubis appeared in 8/25 subjects of group 1, in 5/7 subjects of group 2, in 3/3 subjects of group 3, in 2/2 subjects of group 4. Its appearance was also suspected in 5/25 subjects of group 1.

Trochanter major, trochanter minor, patella, tuberositas tibiae, malleolus medialis tibiae, caput fibulae, malleolus medialis fibulae, ossa tarsi I and *II* were present in none of the subjects of the four groups (0/37).

Caput ossis femoris appeared in 0/25 subjects of group 1, in 1/7 subject of group 2, in 1/3 subjects of group 3, in 2/2 subjects of group 4 (fig. 5); the *condylus lateralis* appeared in 0/25 subjects of group 1, in 1/7 subjects of group 2, in 0/3 subjects of group 3, in 1/2 subjects of group 4; the *condylus medialis* appeared in 0/25 subjects of group 1, in 1/7 subjects of group 2, in 0/3 subjects of group 3, in 1/2 subjects of group 4. *Trochlea femoris* appeared in ½ subjects of group 4.

Figure 5 - Medio-lateral projection of right *os femoris* of a 28-days-old Chihuahua. The ossification centers of *caput ossis femoris,* femoral condyles and tibial proximal epiphysis are evident.

The tibial proximal epiphysis appeared in 0/25 subjects of group 1, in 1/7 subjects of group 2, in 0/3 subjects of group 3, in 2/2 subjects of group 4 (figg. 5-6); *cochlea tibiae* appeared in 0/25 subjects of group 1, in 1/7 subjects of group 2, in 0/3 subjects of group 3, in 1/2 subjects of group 4.

Calcaneus appeared in 25/25 subjects of group 1, in 5/7 subjects of group 2, in 3/3 subjects of group 3, in 2/2 subjects of group 4; *talus* appeared in 12/25 subjects of group 1, in 5/7 subjects of group 2, in 3/3 subjects of group 3, in 2/2 subjects of group 4; *os tarsi centrale* appeared in 0/25 subjects of group 1, in 0/7 subjects of group 2, in 0/3 subjects of group 3, in 2/2 subjects of group 4; *os tarsale III* appeared in 0/25 subjects of group 1, in 0/7 subjects of group 2, in 0/3 subjects of group 3, in 1/2 subjects of group 4; *os tarsale IV* appeared in 0/25 subjects of group 1, in 1/7 subjects of group 2, in 1/3 subjects of group 3, in 2/2 subjects of group 4 (fig. 6) (Table 5).

Figure 6 – Caudo-cranial projection of left *tibia* and *tarsus* of a 28-days-old Chihuahua. The ossification centers of femoral condyles, tibial proximal epiphysis, *cochlea tibiae, calcaneus, talus, os tarsi centrale, ossa tarsalia III* and *IV* are evident.

U-Mann-Whitney test showed high significance between the appearance on radiographs of *caput humeri* and the humeral length, of *os pubis* and femoral length, of *talus* and femoral and tibial lengths. It showed no significance between the appearance on radiographs of *calcaneus* and femoral and tibial lengths. ANOVA showed high significance between the appearance of *corpus ossis accessori* and both radial and ulnar lengths, of *caput ossis femoris* with femoral length, and between *os tarsale IV* and tibial length.

OC/Age	I group (n25)	II group (n7)	III group (n3)	IV group (n2)
Diaphysis	100%	100%	100%	100%
Humeral proximal epiphysis	0%	43%	100%	100%
Trochlea humeri	0%	14%	33%	100%
Capitulum humeri	0%	14%	33%	0%
Epicondylus medialis humeri	0%	14%	0%	0%
Caput radii	0%	0%	0%	50%
Trochlea radii	0%	0%	0%	100%
Tuber olecrani	0%	0%	0%	0%
Caput ulnae	0%	0%	0%	0%
Os carpi radiale	0%	0%	0%	50%
Os carpi intermedium	0%	0%	0%	100%
Os carpi centrale	0%	0%	0%	0%
Os carpi ulnare	0%	0%	0%	100%
Os carpi accessorium	0%	29%	33%	100%
Os carpale I, II, III, IV	0%	14%	0%	50%

Table 4 - Presence of forelimb ossification centers

OC/Age	I group (n25)	II group (n7)	III group (n3)	IV group (n2)
Os ischia	100%	100%	100%	100%
Os pubis	32%	71%	100%	100%
Diaphysis	100%	100%	100%	100%
Caput ossis femoris	0%	14%	33%	100%
Trochanter major femoris	0%	0%	0%	0%
Trochanter minor femoris	0%	0%	0%	0%
Trochlea	0%	0%	0%	50%
Condylus medialis femoris	0%	14%	0%	50%
Condylus lateralis femoris	0%	14%	0%	50%
Patella	0%	0%	0%	0%
Tibial proximal epiphysis	0%	14%	0%	100%
Tuberositas tibiae	0%	0%	0%	0%
Cochlea tibiae	0%	14%	0%	50%
Malleolus medialis tibiae	0%	0%	0%	0%
Calcaneus	100%	71%	100%	100%
Talus	48%	71%	100%	100%
Os tarsi centrale	0%	0%	0%	100%
Os tarsale I	0%	0%	0%	0%
Os tarsale II	0%	0%	0%	0%
Os tarsale III	0%	0%	0%	50%
Os tarsale IV	0%	14%	33%	100%

Table 5 - Presence of hind limb ossification centers

Craniometric and body length measurements

Tables 6-7 show the average values of all the long bones, craniometric and body length measurements on radiographs.

Number	Group	SL (mm)	NW (mm)	CRL (mm)	VCL (mm)	ZW (mm)	CL (mm)
1	1	38,33	25,00	158,53	163,39	25,00	29,00
2	1	36,45	23,85	131,37	129,63	22,68	30,38
3	1	34,37	21,63	126,54	126,47	22,21	25,38
4	1	37,78	27,01	135,85	146,29	25,11	30,46
5	1	35,00	22,00	119,80	126,20	20,67	27,00
6	1	34,33	22,67	125,75	130,88	22,00	25,67
7	1	36,46	22,65	117,09	127,76	20,82	26,50
8	1	39,63	28,67	135,85	146,29	23,77	30,00
9	1	39,29	26,32	136,58	158,49	26,20	30,59
10	1	45,00	25,80	158,53	163,39	27,87	30,60
11	1	38,05	25,15	150,48	158,49	24,50	28,93
12	1	37,26	22,80	131,62	135,45	20,96	28,70
13	1	44,40	25,22	148,79	154,16	25,65	32,28
14	1	38,73	24,22	128,31	126,22	21,87	27,97
15	1	40,81	24,95	129,62	132,22	24,10	30,24
16	1	39,37	25,34	124,43	127,67	24,92	29,76
17	1	33,63	25,47	119,47	123,09	22,23	27,00
18	1	40,03	24,32	126,09	128,55	19,93	29,20
19	1	38,08	22,72	117,09	108,55	19,29	28,29
20	1	42,53	25,23	156,92	155,31	26,40	30,73
21	1	36,35	25,75	124,45	129,53	21,73	29,74
22	1	35,90	27,13	145,51	146,41	25,00	30,52
23	1	36,75	24,64	140,22	150,75	24,09	30,81
24	1	43,73	23,33	154,93	158,78	28,60	32,93
25	1	43,61	31,73	157,33	159,58	29,22	33,81
26	2	41,85	24,17	121,21	130,09	23,53	30,25
27	2	40,32	23,85	119,38	128,40	23,84	29,86
28	2	35,50	25,33	108,54	107,02	21,20	27,67
29	2	51,33	35,23	177,68	189,63	31,67	39,67
30	2	43,27	27,09	143,61	149,35	25,86	31,34
31	2	45,53	30,00	132,62	134,61	24,03	32,13
32	2	40,00	29,23	134,32	138,75	23,50	29,17
33	3	43,13	31,87	152,43	150,91	27,07	33,07
34	3	42,50	36,60	139,82	136,69	30,40	36,10
35	3	44,01	36,35	168,57	180,50	29,80	35,55
36	4	58,01	40,96	177,66	166,67	29,49	45,97
37	4	60,08	46,82	195,17	197,43	39,27	48,60

Table 6 - Average values of radiographic measurements (part 1)

SK= skull length, NW= neurocranium width, CRL=crown-rump length, VCL=vertebral column length
ZW= zigomatic width, CL= cranial length

Number	Group	VL (mm)	HL (mm)	RL (mm)	UL (mm)	FL (mm)	TL (mm)
1	1	9,33	14,67	11,67	14,00	14,67	12,23
2	1	6,90	15,38	13,05	14,61	15,44	14,10
3	1	8,52	13,47	10,54	10,62	14,23	11,44
4	1	7,17	14,51	11,66	13,58	14,56	13,01
5	1	8,00	14,00	10,88	12,72	13,39	11,86
6	1	10,00	13,00	10,00	12,00	13,00	11,00
7	1	7,70	16,52	12,94	14,49	16,51	11,70
8	1	7,97	16,00	13,33	16,33	17,00	15,33
9	1	7,81	16,41	13,80	15,83	16,72	14,25
10	1	14,40	16,67	13,10	14,67	16,30	14,13
11	1	8,51	16,95	13,75	15,58	16,67	14,57
12	1	7,24	15,42	12,40	14,30	14,34	13,55
13	1	11,39	15,90	13,34	15,49	16,53	14,66
14	1	6,99	11,69	10,82	12,61	9,90	11,87
15	1	10,55	15,91	12,36	14,26	16,75	13,85
16	1	9,66	17,05	13,07	14,82	18,18	14,82
17	1	5,03	13,17	10,53	11,53	13,33	11,17
18	1	10,48	17,67	13,62	16,26	17,44	15,41
19	1	9,76	16,53	13,24	15,14	12,75	15,07
20	1	11,97	19,63	16,50	18,40	19,87	18,67
21	1	6,90	15,35	12,73	14,59	15,76	14,08
22	1	7,84	17,06	13,46	15,52	16,79	14,18
23	1	6,40	16,03	13,02	14,72	16,46	13,99
24	1	11,07	15,80	12,93	15,27	16,53	14,73
25	1	7,98	17,65	14,91	17,38	17,85	15,41
26	2	9,18	17,97	14,19	15,80	17,28	16,21
27	2	8,99	17,85	13,97	15,94	17,67	15,99
28	2	7,60	15,93	12,30	14,93	15,20	13,33
29	2	12,33	19,33	16,00	20,00	20,00	16,67
30	2	11,04	16,35	13,07	15,46	16,29	14,44
31	2	8,00	16,63	14,20	16,33	16,80	16,47
32	2	10,00	14,40	12,20	13,90	14,23	13,37
33	3	10,17	16,17	13,67	16,23	17,13	15,20
34	3	7,83	16,53	14,00	16,43	17,97	15,87
35	3	7,42	19,85	16,58	19,00	18,35	16,69
36	4	16,82	30,28	25,80	30,48	32,51	29,84
37	4	6,86	22,60	18,57	22,56	24,64	20,78

Table 7 - Average values of radiographic measurements (part 2)

VL= viscero-cranial length, HL= humeral length, RL= radial length, UL= ulnar length, FL= femoral length, TL= tibial length

Friedman's test showed that the three measurements of each length and width are repeatable and the mean values were employed in the subsequent statistical analysis.

Pearson's correlation coefficient[2] was employed to correlate the radiographic measures between them and with body mass and days of age. The correlations resulted mostly highly significant with P<0,01 (table 8). The correlations between viscero-cranial length and cranial length, and between viscero-cranial length and crown-rump length resulted significant with P<0,05 (table 8).

The correlations between viscero-cranial length and age, viscero-cranial length and neurocranium width, viscero-cranial length and zigomatic width, viscero-cranial length and vertebral column lengths were not significant (table 8).

		A	W	SL	NW	CRL	VCL	ZW	CL	VL	HL	RL	UL	FL	TL
A	Pearson's correlation	1	,551**	,761**	,765**	,589**	,488**	,695**	,823**	,195	,702**	,730**	,747**	,699**	,721**
	p		,000	,000	,000	,000	,002	,000	,000	,248	,000	,000	,000	,000	,000
	N	37	37	37	37	37	37	37	37	37	37	37	37	37	37
W	Pearson's Correlation	,551**	1	,783**	,625**	,924**	,901**	,828**	,768**	,447**	,613**	,649**	,669**	,637**	,583**
	p	,000		,000	,000	,000	,000	,000	,000	,006	,000	,000	,000	,000	,000
	N	37	37	37	37	37	37	37	37	37	37	37	37	37	37
SL	Pearson's Correlation	,761**	,783**	1	,721**	,806**	,723**	,824**	,935**	,527**	,798**	,827**	,856**	,813**	,825**
	p	,000	,000		,000	,000	,000	,000	,000	,001	,000	,000	,000	,000	,000
	N	37	37	37	37	37	37	37	37	37	37	37	37	37	37
NW	Pearson's Correlation	,765**	,625**	,721**	1	,589**	,468**	,647**	,793**	,179	,635**	,672**	,703**	,574**	,658**
	p	,000	,000	,000		,000	,003	,000	,000	,289	,000	,000	,000	,000	,000
	N	37	37	37	37	37	37	37	37	37	37	37	37	37	37
CRL	Pearson's Correlation	,589**	,924**	,806**	,589**	1	,954**	,881**	,821**	,406*	,623**	,667**	,694**	,656**	,609**
	p	,000	,000	,000	,000		,000	,000	,000	,013	,000	,000	,000	,000	,000
	N	37	37	37	37	37	37	37	37	37	37	37	37	37	37
VCL	Pearson's Correlation	,488**	,901**	,723**	,468**	,954**	1	,859**	,738**	,305	,530**	,564**	,595**	,574**	,482**
	p	,002	,000	,000	,003	,000		,000	,000	,066	,001	,000	,000	,000	,003
	N	37	37	37	37	37	37	37	37	37	37	37	37	37	37

ZW	Pearson's Correlation	,695**	,828**	,824**	,647**	,881**	,859**	1	,873**	,241	,577**	,608**	,639**	,652**	,567**
	p	,000	,000	,000	,000	,000	,000		,000	,151	,000	,000	,000	,000	,000
	N	37	37	37	37	37	37	37	37	37	37	37	37	37	37
CL	Pearson's Correlation	,823**	,768**	,935**	,793**	,821**	,738**	,873**	1	,333*	,811**	,845**	,878**	,842**	,828**
	p	,000	,000	,000	,000	,000	,000	,000		,044	,000	,000	,000	,000	,000
	N	37	37	37	37	37	37	37	37	37	37	37	37	37	37
Viscero-cranial L.	Pearson's Correlation	,195	,447**	,527**	,179	,406*	,305	,241	,333*	1	,534**	,510**	,510**	,519**	,545**
	p	,248	,006	,001	,289	,013	,066	,151	,044		,001	,001	,001	,001	,000
	N	37	37	37	37	37	37	37	37	37	37	37	37	37	37
HL	Pearson's Correlation	,702**	,613**	,798**	,635**	,623**	,530**	,577**	,811**	,534**	1	,982**	,969**	,963**	,959**
	p	,000	,000	,000	,000	,000	,001	,000	,000	,001		,000	,000	,000	,000
	N	37	37	37	37	37	37	37	37	37	37	37	37	37	37
RL	Pearson's Correlation	,730**	,649**	,827**	,672**	,667**	,564**	,608**	,845**	,510**	,982**	1	,987**	,949**	,977**
	p	,000	,000	,000	,000	,000	,000	,000	,000	,001	,000		,000	,000	,000
	N	37	37	37	37	37	37	37	37	37	37	37	37	37	37
UL	Pearson's Correlation	,747**	,669**	,856**	,703**	,694**	,595**	,639**	,878**	,510**	,969**	,987**	1	,943**	,967**
	p	,000	,000	,000	,000	,000	,000	,000	,000	,001	,000	,000		,000	,000
	N	37	37	37	37	37	37	37	37	37	37	37	37	37	37
FL	Pearson's Correlation	,699**	,637**	,813**	,574**	,656**	,574**	,652**	,842**	,519**	,963**	,949**	,943**	1	,935**
	p	,000	,000	,000	,000	,000	,000	,000	,000	,001	,000	,000	,000		,000
	N	37	37	37	37	37	37	37	37	37	37	37	37	37	37
TL	Pearson's Correlation	,721**	,583**	,825**	,658**	,609**	,482**	,567**	,828**	,545**	,959**	,977**	,967**	,935**	1
	p	,000	,000	,000	,000	,000	,003	,000	,000	,000	,000	,000	,000	,000	
	N	37	37	37	37	37	37	37	37	37	37	37	37	37	37

Table 8 - Pearson's correlation radiographic measurements - ** P<0,01 * P<0,05

A= age, W= weight, SK= skull length, NW= neurocranium width, CRL=crown-rump length, VCL=vertebral column length ZW= zigomatic width, CL= cranial length, VL= viscero-cranial length, HL= humeral length, RL= radial length, UL= ulnar length, FL= femoral length, TL= tibial length

Densitometric analysis

Table 9 shows the bone mineral densities obtained from each specimen.
BMD was calculated on a minimum of two samples for each group: 4 specimens of group 1, 2 specimens of group 2, 3 specimens of group 3, 2 specimens of group 4 (Table 9).

The minimum value of BMD of *radius* and *ulna* was 0,0549 g/cm2 and the minimum value of BMD of *os femoris* was 0,0626 g/cm2. These values belong to the youngest dog of the study, who is a Chihuahua.
The maximum value of BMD of *radius* and *ulna* was 0,2024 g/cm2 and the maximum value of BMD of *os femoris* was 0,2539 g/cm2. These values belong to the oldest dog of the study, who is a 28-days-old Chihuahua.
The mean BMD of *radius* and *ulna* was 0,1068 g/cm2 in group 1, it was 0,0923 g/cm2 in group 2, it was 0,1372 g/cm2 in group 3 and it was 0,1886 g/cm2 in group 4.
The mean BMD of *os femoris* was 0,1604 g/cm2 in group 1, it was 0,1377 g/cm2 in group 2, it was 0,1893 g/cm2 in group 3 and it was 0,2280 g/cm2 in group 4.

Number	Group	BMD Radius-Ulna (g/cm2)	BMD Femur (g/cm2)
5	1	0,0549	0,0626
29	1	0,125	0,1730
30	1	0,1381	0,1910
31	1	0,152	0,2150
34	2	0,0477	0,0704
35	2	0,1455	0,2049
39	3	0,131	0,185
40	3	0,157	0,167
41	3	0,1237	0,2158
42	4	0,173	0,2020
43	4	0,2042	0,2539

Table 9 - Bone mineral densities of *radius* and *ulna* and *os femoris*

Sperman bivariate correlation showed high significance between the general bone mineral density of *radius* and *ulna* and both radial and ulnar lengths, and between the general bone mineral density of *os femoris* and femoral length.

Anatomical and histological analysis

Anatomical and histological studies were performed on 5 subjects of group 1, 4 subjects of group 2, 3 subjects of group 3, 2 subjects of group 4, randomly chosen between the total of subjects enrolled (tables 10-11).

Evaluation of ossification centers

Histological and histochemical analysis confirmed the presence of the ossification centers of the epiphyses of long bones and of the carpal and tarsal bones identified by X-rays images. On the basis of the observation made in this study and of the results obtained previously by Rivas and Shapiro in the rabbit (Rivas and Shapiro, 2002), they were classified as ossification center type 1 (OCT1), type 2 (OCT2) and type 3 (OCT3); 2) described the presence of ossification like centers that were not identified by radiographic analysis (ossification center type 0 - OCT0) (fig. 7 A, B, C, D).

Ossification center type 0 (OCT0) in fact showed hypertrophic lacunae containing hypertrophic or flattened or degenerate chondrocytes. ECM surrounding lacunae had occasionally a granular aspect (fig. 7A).

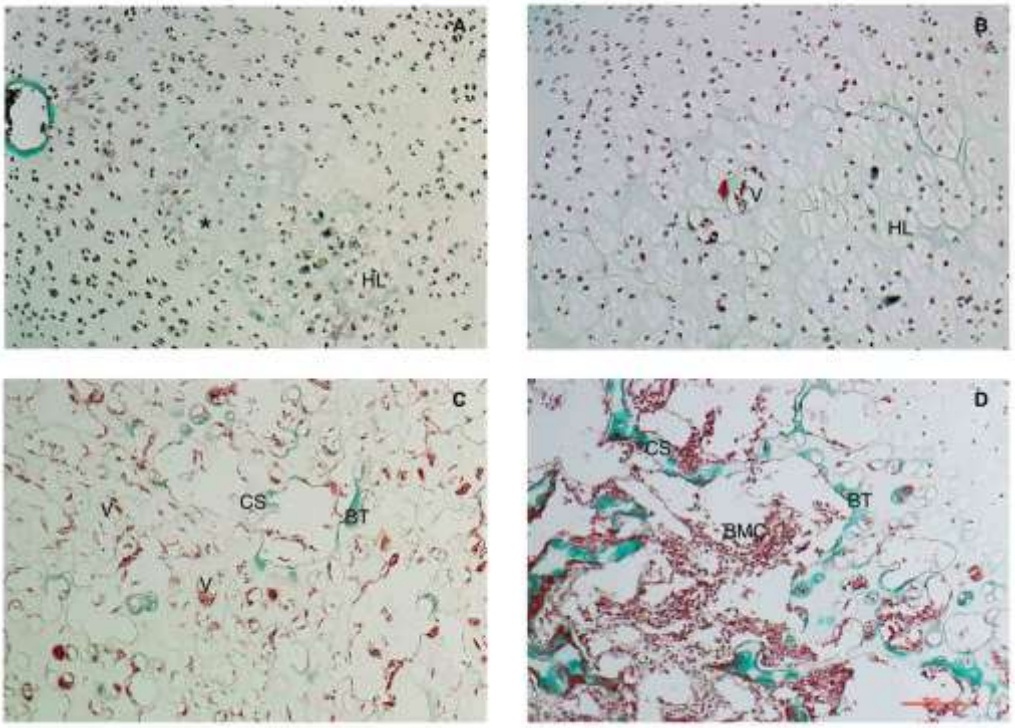

Figure 7 - Histological sections showing A(OCT1); B (OCT2); C (0CT2); D(OCT3). HL(Hypertrophic Lacunae); * (granular ECM); V (Vessel); CS (Cartilage Septa); BT(Bone Tissue); BMC(Bone Marrow Cells). Masson Trichromic Staining. Scale Bar 100 μm .

In OCT1, chondrocytes and lacunae showed the same aspect of OCT0; some lacunae appeared empty and confluent and the vessels of the cartilage canals started to invade cell lacunae; (fig 7B); in the long bone OCT1 showed a spherical organization and the epiphyseal cartilage immediately peripheral to the enlarged lacunae organized the growth plate of the secondary ossification center (fig. 8).

Figure 8 - Fig 2. Histological longitudinal section through the *trochlea humeri* of a 10-days-old Maltese. EE staining. Scale Bar 1000 μm.

In OCT2, most of the lacunae were fused into larger space of irregular size and

orientation, delimited by septa of cartilage ECM surrounding them. Vessels invaded lacunae. Occasionally it was possible to observe neo-formed bone tissue closed to the septa (fig 7C). Long bones OCT2 showed a spherical organization (fig. 9).

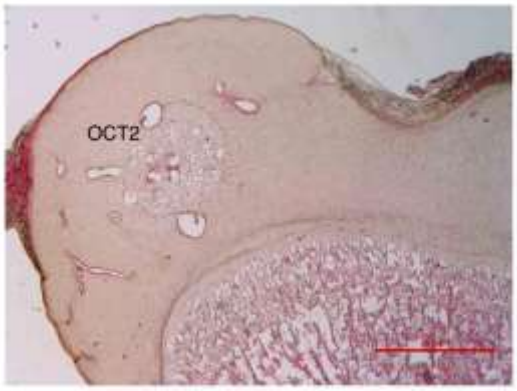

Figure 9 - Histological longitudinal section through the *caput ossis femoris* of a 15-days-old Maltese. EE staining. Scale Bar 1000 μm.

OCT3 was characterized by an interweaving of septa covered by neo formed bone tissue and cells of ossification front. Bone marrows cells were localized inside the spaces between the septa (Fig 7D). In *caput humeri* and in *caput ossis femuris* there was also a change in the shape of the center from spherical to hemispherical (fig. 10).

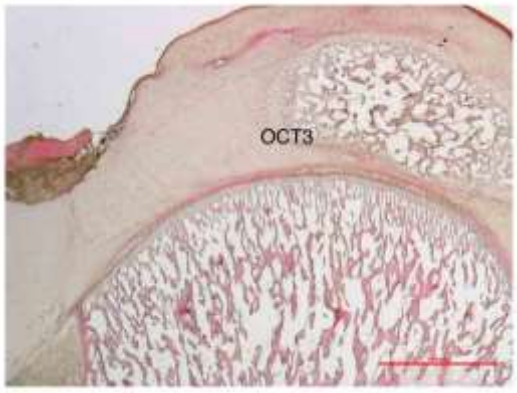

Figure 10 - Histological longitudinal section through the *caput ossis femoris* of a 28-days-old Chihuahua. EE staining. Scale Bar 1000 μm.

As indicated in tables 10-11, OCT0, OCT1 OCT2 and OCT3 were variously distributed within the bones of the four groups observed. For each bone a single ossification center was identified, with the exception of *os carpi intermedioradiale* where, in the same bone, two OCT2 were encased in a unique cartilagineus mold

(fig. 11).

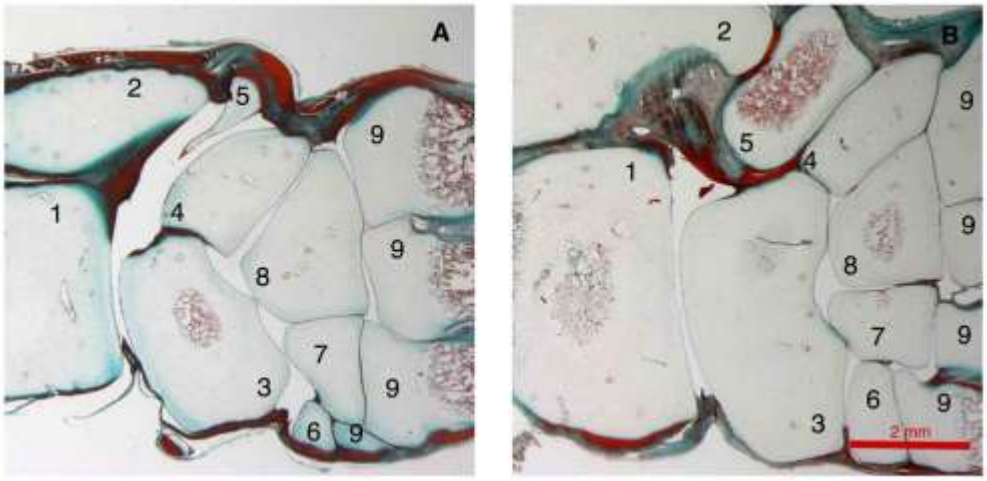

Figure 11 - Histological dorsal sections of the *carpus* of a 28-days-old Chihuahua performed at 2 different planes. 1(*Radius*); 2(*Ulna*); 3 (*os carpi intermedioradiale*); 4 (*os carpi ulnare*); 5 (*os carpi accessorium*); 6 (*os carpale II*); 7 (*os carpale III*); 8 (*os carpale IV*); 9 (*Metacarpus*). Masson trichromic staining. Scale Bar 2000 μm.
In the intermedioradial carpal boned is visible on of the two ossification centers.

In both the epiphyses of the long bones and in the *ossa carpi* and *tarsi* and the appearance of OCT0, OCT1 and OCT2 was preceded by various grades of hypertrophy of the chondrocytes (fig. 6B). Finally, in absence of ossification centers and hypertrophic condrocytes, cartilage models were formed by rounded and proliferative chondrocytes (fig. 12A).

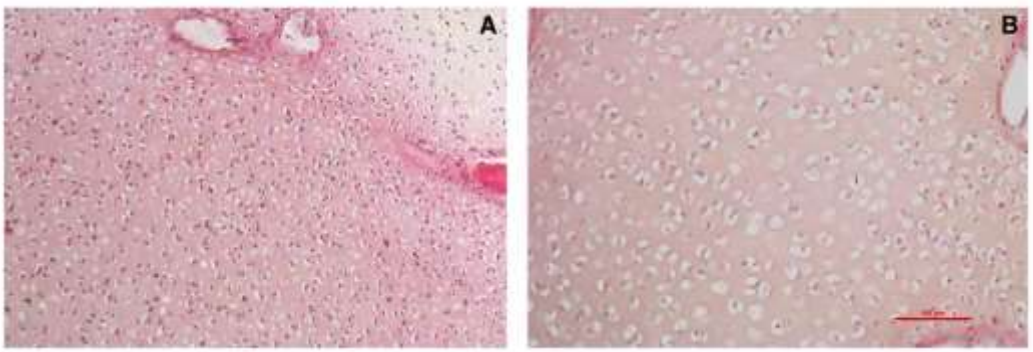

Figure 12 - Histological sections showing A: rounded proliferative chondrocytes;
B: hypertrophic chondrocytes enclosed in enlarged lacunae. EE Staining. Scale Bar 100 μm.

Number	2	17	23	24	25	28	29	31	32	33	34	35	36	37
Group	1	1	1	1	1	2	2	2	2	3	3	3	4	4
Humeral proximal epiphysis							OCT2	OCT2	OCT2	OCT2	OCT3	OCT2	OCT3	OCT3
Trochlea humeri							OCT2				OCT0		0CT2	OCT3
Capitulum humeri							OCT2				OCT0	OCT2		
Epicondylus medialis humeri							OCT2							
Caput radii													OCT2	OCT2
Trochlea radii							OCT1						OCT2	OCT2
Tuber olecrani														
Caput ulnae														
Os carpi radiale								OCT0			OCT0		OCT2	OCT2
Os carpi intermedium								OCT0			OCT0		OCT2	OCT2
Os carpi centrale														
Os carpi ulnare													OCT1	OCT1
Os carpi accessorium							OCT1	OCT1			OCT2		OCT3	OCT3
Os carpale I,II,III,IV											IV		I: OCT1	III: OCT1, IV:OCT2

Table 10 - Histological analysis of the ossification centers of the forelimb

OCT0 = ossification center type 0, OCT1 = ossification center type 1, OCT2 = ossification center type 2, OCT3 = ossification center type 3

Number	2	17	23	24	25	28	29	31	32	33	34	35	36	37
Group	1	1	1	1	1	2	2	2	2	3	3	3	4	4
Caput ossis femoris							OCT2			OCT1	OCT2		OCT3	OCT3
Trochanter major femoris														
Trochanter minor femoris														
Trochlea ossis femoris													OCT3	
Condylus lateralis femoris														OCT 3
Condylus medialis femoris														OCT3
Tibial proximal epiphysis														
Tuberositas tibiae														
Malleolus mediali tibiae														
Cochlea tibiae						OCT2							OCT2	OCT2
Calcaneus	OCT2	OCT2	OCT2	OCT2	OCT2	OCT3	OCT2	OCT3	OCT3	OCT3	OCT3	OCT3	OCT3	OCT3
Talus	OCT2		OCT2	OCT2	OCT2	OCT3	OCT2	0CT3	OCT3	OCT3	OCT3	OCT3	OCT3	OCT3
Os tarsi centrale													OCT2	OCT2
Os tarsale I														
Os tarsale II														
Os tarsale III													OCT1	OCT1
Os tarsale IV						OCT1							OCT1	OCT1

Table 11 - Histological analysis of the ossification centers of the hind limb

OCT0 = ossification center type 0, OCT1 = ossification center type 1, OCT2 = ossification center type 2, OCT3 = ossification center type 3

Anatomical measurements

Table 12 shows the average values of all skull length, neurocranium width, crown-rump, vertebral column, humeral, radial, femoral and tibial lengths of the cadavers (table 12).

Number	Group	SL (mm)	NW (mm)	CRL (mm)	VCL (mm)	HL (mm)	RL (mm)	FL (mm)	TL (mm)
2	1	40,83	23,77	136,10	141,00	25,60	25,60	24,20	24,60
17	1	36,63	24,37	124,87	127,17	23,67	17,17	19,53	17,80
23	1	41,57	25,60	147,33	164,67	23,73	20,73	22,13	24,13
24	1	45,50	26,27	148,33	168,67	22,43	26,33	22,00	24,50
25	1	45,00	38,87	152,67	159,67	26,40	24,83	25,17	26,60
28	2	39,20	24,80	110,67	119,10	19,87	20,00	18,37	20,03
29	2	56,20	36,67	250,00	199,33	30,47	29,23	26,40	32,13
31	2	42,70	31,23	126,20	125,43	21,73	19,33	22,67	21,33
32	2	41,63	30,70	120,60	122,27	18,73	16,90	21,73	19,07
33	3	49,03	31,53	158,33	155,67	26,30	22,73	24,73	27,90
34	3	48,73	38,57	142,60	147,40	25,03	24,23	24,17	27,60
35	3	32,00	35,30	180,67	193,00	29,37	27,50	31,67	29,83
36	4	63,87	40,30	188,67	185,33	36,53	35,47	35,17	36,47
37	4	61,87	46,83	203,00	210,00	34,83	37,83	31,27	33,50

Table 12 - Average values of anatomical measurements

SK= skull length, NW= neurocranium width, CRL=crown-rump length, VCL=vertebral column length, HL= humeral length, RL= radial length, FL= femoral length, TL= tibial length

Friedman's test showed that the three measurements of each length and width are repeatable and the mean values were employed in the subsequent statistical analysis. Pearson's correlation coefficient[2] was employed to correlate the anatomical measurements between them and with body mass and days of age. Most of the correlations resulted hightly significant with $P<0,01$ (table 13). The correlations between skull length and crown-rump length, skull length and vertebral-column length, skull length and femoral length, skull length and age, neurocranium width and crown-rump length, vertebral-column length and age, humeral length and age, radial length and age resulted significant with $P<0,05$. The correlations between crown-rump length and age were not significant (table 13). Sperman bivariate correlation was employed to correlate radiographic measures with the anatomical measurements. The correlations resulted almost hightly significant.

		W	SL	NW	CRL	VCL	HL	RL	FL	TL	A
W	Pearson's Correlation	1	,677**	,819**	,909**	,913**	,894**	,839**	,887**	,897**	,751**
	p		,008	,000	,000	,000	,000	,000	,000	,000	,002
	N	14	14	14	14	14	14	14	14	14	14
SL	Pearson's Correlation	,677**	1	,699**	,644*	,578*	,719**	,758**	,586*	,755**	,568*
	p	,008		,005	,013	,030	,004	,002	,028	,002	,034
	N	14	14	14	14	14	14	14	14	14	14
NW	Pearson's Correlation	,819**	,699**	1	,646*	,670**	,742**	,735**	,765**	,777**	,799**
	p	,000	,005		,013	,009	,002	,003	,001	,001	,001
	N	14	14	14	14	14	14	14	14	14	14
CRL	Pearson's Correlation	,909**	,644*	,646*	1	,904**	,805**	,765**	,702**	,842**	,467
	p	,000	,013	,013		,000	,001	,001	,005	,000	,092
	N	14	14	14	14	14	14	14	14	14	14
VCL	Pearson's Correlation	,913**	,578*	,670**	,904**	1	,845**	,866**	,795**	,881**	,566*
	p	,000	,030	,009	,000		,000	,000	,001	,000	,035
	N	14	14	14	14	14	14	14	14	14	14
HL	Pearson's Correlation	,894**	,719**	,742**	,805**	,845**	1	,915**	,914**	,931**	,654*
	p	,000	,004	,002	,001	,000		,000	,000	,000	,011
	N	14	14	14	14	14	14	14	14	14	14
RL	Pearson's Correlation	,839**	,758**	,735**	,765**	,866**	,915**	1	,859**	,921**	,661*
	p	,000	,002	,003	,001	,000	,000		,000	,000	,010
	N	14	14	14	14	14	14	14	14	14	14
FL	Pearson's Correlation	,887**	,586*	,765**	,702**	,795**	,914**	,859**	1	,907**	,772**
	Sig. p	,000	,028	,001	,005	,001	,000	,000		,000	,001
	N	14	14	14	14	14	14	14	14	14	14
TL	Pearson's Correlation	,897**	,755**	,777**	,842**	,881**	,931**	,921**	,907**	1	,682**

	p	,000	,002	,001	,000	,000	,000	,000	,000		,007
	N	14	14	14	14	14	14	14	14	14	14
A	Pearson's Correlation	,751**	,568*	,799**	,467	,566*	,654*	,661*	,772**	,682**	1
	p	,002	,034	,001	,092	,035	,011	,010	,001	,007	
	N	14	14	14	14	14	14	14	14	14	14

Table 13 - Pearson's correlation between anatomical measurements, age and weight - ** P<0,01 * P<0,05

A= age, W= weight, SK= skull length, NW= neurocranium width, CRL=crown-rump length, VCL=vertebral column length ZW= zigomatic width, CL= cranial length, VL= viscero-cranial length, HL= humeral length, RL= radial length, FL= femoral length, TL= tibial length

Discussion

Skeleton evaluation to estimate the age of unidentified people, corpses and remains has a long tradition in forensic science. Criteria that can be applied to investigate skeletons of children and adolescents are tooth mineralization status, length of longitudinal bones measurement and developmental status of the epiphysis (Cunha et al., 2009; Schmeling et al., 2007). Even if these criteria would be predetermined and standardized, the individual variability should be considered, especially in pubertal stage, because at all stages of life there are people whose body is biologically younger or older than their chronological age (Cunha et al., 2009). This aspect, in human being, is an obstacle almost impossible to overcome if the age estimation must be carried out for legal purposes. In man, skeletal age assessment by means of a radiograph of the left hand is a given common currency in legal practice. Radiograph evaluation relies on the recognition of primary and secondary ossification centers, degree of epiphyseal plates ossification, their degree of development, increase in size and change in shape of each bones, with low exposure of the patient to ionizing radiation (Schmidt et al., 2013a). Images are subsequently compared with radiographs obtained from children with known age. It's well known and accepted that references are not available for all ethnic groups, and estimation of the biological age of a man represents an average age of a man in that group of age and of that sex without considering the individual variability(Cunha et al., 2009; Franklin, 2010).

These issues are even more important in Veterinary Medicine because as in other mammals, physical development of the dog, from puppy to adult, is associated with deep skeleton modifications, which quickly occur in a shorter period of time. Moreover there are up to 400 breed dogs with great heteromorphy to each others: body weight can vary 100-fold from 1-kg (Chihuahua) to 115-kg (St. Bernard) (Burger, 1994). The time taken for a

growing puppy to achieve adult body weight also varies considerably with larger breeds having a longer growth period than smaller breeds. Thus although a toy or small-breed dog may be considered an adult from 9 months of age, adulthood in the largest breeds is not achieved until 15 months of age (Hawthorne et al., 2004). Puppies are usually sold at the age of 9-11 weeks and for both the breeder and the potential owner the prospective physical development may be relevant to choose a puppy. "Even if during postnatal development growing problems may occur, it's important to have reference values for the postnatal growth" (Helmsmuller et al., 2013).

Individual and environmental factors could be considered the same for both Human and animals, but in Veterinary Medicine nutritional factors can be considered another variable, because bitches can be fed differently between different breeders, litters are numerous and every puppy is fed in a different way compared with the others (Eilts et al., 2005; Vanden Berg-Foels et al., 2006).
To date, radiographic evaluation of the appearance and fusion of ossification centers in limbs bones is the most widespread method for age estimation in growing dogs. If the technical approach is simple, cheap, repeatable, available for mass screening and *postmortem* too, interpretation of data can be hard due to the lack of detailed and standardized references. Previous data in fact are often not homogeneous for breeds, anatomical compartments and timing of investigation. Textbooks of Veterinary Radiology as well as Veterinary Anatomy suggest table of the appearance and fusion of ossification centers. Data from different Authors (Chapman, 1965; Hare, 1959a, b, 1960a, c, d, 1961; Scholotthaurer, 1952; Smith, 1960a; Smith, 1960b) have been reported in the textbook "Veterinary Radiology" by Carlson (Carlson, 1967) and in the "Textbook of Small Animal Orthopaedics" (Newton, 1985), and German Shepherd dog, Bulldog, Collie and Beagle were considered. The same bibliographic sources, implemented by the observations of others Authors

(Hare, 1960a, c; Pomriaskinsky- Kobozieff and Kobozieff, 1954; Sumner-Smith, 1966; Ticer, 1984) have been employed by de Lahunta and Habel (De Lahunta and Habel, 1986) in "Applied Veterinary Anatomy" and subsequently reported in the "Textbook of Veterinary Anatomy" (Dyce et al., 2010).

A complete table dating appearance and fusion of ossification centers of forelimb and hind limb in German Shepherd dog has been presented by Schebitz (Schebitz and Wilkens, 1978), starting from previous works, however neither the number of dogs enrolled nor the interval of examinations were indicated.

Tables on ossification centers have also been published by Ticer, in "Radiographic Technique in Veterinary practice" (Ticer, 1984), they have been reported by Kealy in "Diagnostic Radiology of the dog and the cat" (Kealy, 1987) } and by Burk and Feeney in "Small Animal Radiology and Ultrasound: A Diagnostic Atlas and Text" in 1996 (Ronald L. Burk, 1996) but, again, number of dogs and the breeds examined were not considered. Ticer's observations (Ticer, 1984), implemented by observations of Sumner-Smith (Sumner-Smith, 1966), have been recently included by Dennis et al. (Dennis et al., 2010) in "Handbook of Small Animal Radiology and Ultrasound Techniques and differential diagnoses".

From 1973 most of the Authors focused their attention on ossification centers of the long limb bones and on the pelvis. Usually data did not improve previous knowledge on age determination, but consolidate previous observations. Most of them were aimed to assess the timing of ossification of bones and skeletal growth with the onset of pathologies, but this topic has not been the subject of this study. Therefore they are focused on single breeds and for the most part, on dogs of medium and large size (Conzemius et al., 1994; Hedhammar et al., 1974b; Madsen et al., 1991; Todhunter et al., 1997; Vanden Berg-Foels et al., 2011; Vanden Berg-Foels et al., 2006).

The most investigated breed is the Beagle (Chapman, 1965; Frazho et al., 2010; Fukuda and Matsuoka, 1980; Hare, 1961; Helmsmuller et al., 2013; Yonamine et al., 1980; Zoetis et al., 2003) probably because he often is employed as laboratory animal. German Shepherd dog has been studied too, probably due to the high prevalence and spread of this breed in canine population (Bressou et al., 1957; Frazho et al., 2010; Hare, 1961; Schebitz and Wilkens, 1978). Some studies have been carried out on Greyhound too (Gustaffson et al., 1975; Smith, 1960a; Smith, 1960b), while some Authors focused their attention on others breeds, but often they enrolled only a small number of subjects or they focused their attention only on some anatomical compartments or on the onset of skeletal pathologies (Breit et al., 2004; Frazho et al., 2010; Mahler and Havet, 1999a; Todhunter et al., 1997).

Literature analysis reported above underlines the lack of systematic papers concerning the radiographic appearance of ossification centers and their fusion in toy-dog breeds. Moreover there are even less papers regarding this topic in newborn dogs. Our work described for the first time the appearance of ossification centers in toy-dog breeds during the first month of life. Radiographic investigation partially confirm what previously described in medium and large size dogs, therefore differences observed must be considered as peculiar characteristics of toy-dog breeds.

Before discussing the results of radiographic investigations, it is necessary to discuss the technical approach. In this study, two different computed radiology (CR) systems are employed with the same x-ray tube. The spatial resolution of the radiological system depends first of all on the size of the focal spot, which in the system employed is 0.6 mm. This value is the limit beyond which it is better not to go in order to avoid a significant decrease in the quality of the images. No difference between two different CR systems employed were detected, even if radiographs obtained from FCR CapsulaX (FUJI) showed a

slightly better contrast resolution, due to a better performance of the Fuji hardware and software systems.

As showed in table 4-5, we observed that all the diaphysis of the bones of the limbs were present in all the subjects of the four groups since their birth, as previous studies previously reported (Chapman, 1965; Evans and Miller, 2013; Hare, 1961; Ticer, 1984; Yonamine et al., 1980).

Clavicula showed a very heterogeneous behavior, but it's not possible to make a comparison with data previously reported regarding medium and big size dogs because other Authors didn't mentioned it in their radiographic papers (Chapman, 1965; Hare, 1959b, 1961; Smith, 1960a; Smith and Allcock, 1960). Only Evans and Miller (Evans and Miller, 2013) reported that it ossifies at 28 days of pregnancy and that it is one of the frist four bones that appears in the embryo.

The body of *scapula* was present in all the subjects of the groups, while *tuberculum supraglenoidale* wasn't evident in this study, in agreement with Literature (Chapman, 1965; Hare, 1959b, 1961; Yonamine et al., 1980).

Humeral proximal epiphysis was constant starting from the third week of age, while it was evident in the 43% of the subjects of the second group. These data are homogeneous with the data reported in most of the previous studies (Chapman, 1965; Fukuda and Matsuoka, 1980; Ticer, 1984; Zoetis et al., 2003), while Hare reported its appearance between 3 and 7 days of age in German Shepherd dogs and Collie (Hare, 1959b, 1961). Furthermore, increasing age humeral head becomes more hemispheric, resembling the final shape of the bony epiphysis.

Trochlea humeri showed a less homogeneous appearance; it was not evident in group 1, it was not constant in groups 2 and 3, and it was radiographically and histologically evident in 100% of the subjects of group 4. Our radiographic data agree with some of the previous papers (Chapman, 1965; Yonamine et al., 1980; Zoetis et al., 2003) and with what Hare reported in Collie, Bulldog, Beagle dogs

and in dogs of not specified breeds (Hare, 1959b, 1961). Conversely, Hare reported a later appearance of this ossification center only in the German Shepherd Dog (30-46 days of age) (Hare, 1961).

Appearance of *capitulum humeri* showed a similar behavior, but it was less homogeneous with data of Literature. In fact, it was not evident in group 1, it was not constant in groups 2 and 3, and it was not evident in the subjects of group 4. Radiographic data are quite heterogeneous but they agree with what reported by Hare, who described its appearance in the German Shepherd dog between 30 and 46 days of age (Hare, 1961), and Yonamine et al., who reported its appearance between 30 and 60 days of age in the Beagle dog (Yonamine et al., 1980). Nevertheless, other Authors reported an earlier appearance of this ossification center (14-21 days of age in different breeds (Hare, 1959b); 10-13 days of age in Collie, 15-17 days of age in Bulldogs, 14-21 days of age in Beagle (Hare, 1961); 18 days of age in Beagle dog (Chapman, 1965), 14-21 days of age in non specified breed (Ticer, 1984)).

Epicondylus medialis wasn't evident in this study, in agreement with Literature. Previous papers, in fact, described a tardive appearance of this ossification center (Chapman, 1965; Hare, 1959b, 1961). In our study it was evident only in subject n. 29 (10 days old Maltese) that showed an early appearance of most of the nuclei observed both in the hind limb and forelimb.

In a German text book of Anatomy (Ellenberger and Hermann, 1943), and in the old work of Lesbre et Al. (Lesbre, 1897) both cited by Hare (Hare, 1961) however, it has been described an independent ossification center for the greater tubercle, even if the same Author was not able to confirm this information.

Marcellin-Little was the first Author who investigated humeral distal epiphysis in Spaniel breed dogs because these breeds showed high incidence of fractures of the distal humeral condyles (Marcellin-Little et al., 1994). Authors hypothesized that a heritable condition resulting in incomplete ossification of the humeral condyles predisposes several Spaniel breeds to fracture (Marcellin-

Little et al., 1994). Even in recent times, other Authors employed different techniques to better evaluate this condition (Carrera et al., 2008; Martin et al., 2010; Piola et al., 2012).

Caput radii appeared only in 50% of the subjects of group 4. This behavior is less homogeneous compared with Literature: it agrees with some Authors (Alvarado Morillo, 2007; Chapman, 1965; Hare, 1959b; Yonamine et al., 1980), while Hare reported that it appears between 15 and 30 days of age in German Shepherd dog, between 21 and 26 days of age in Collie and between 21 and 28 days of age in Beagles, Fukuda and Matsuoka reported that it appears at 14 days of age (Fukuda and Matsuoka, 1980; Hare, 1961) and Ticer between 21 and 35 days of age (Ticer, 1984).

Trochlea radii was not evident radiographically in groups 1, 2, 3 and it was constantly evident starting from the fourth week of age. Its appearance agree with data reported by Hare in Bulldog and Beagle dogs (Hare, 1961) and in different breeds (Hare, 1959b), and by Ticer (Ticer, 1984). Conversely, Pomriaskinsky-Kobozieff and Kobozieff described its appearance between 12 and 15 days of age in different breeds, Hare described its appearance between 10 and 22 days of age in German Shepherd dog and between 11 and 21 days of age in Collie, Fukuda and Matsuoka reported that it appears at 14 days of age in Beagle (Fukuda and Matsuoka, 1980; Hare, 1959b, 1961; Pomriaskinsky-Kobozieff and Kobozieff, 1954).

Tuber olecrani and *caput ulnae* did not appear in any subjects in this study and these data agree completely with Literature, in fact papers reported a later appearance of this ossification center (Chapman, 1965; Fukuda and Matsuoka, 1980; Hare, 1959b, 1961; Pomriaskinsky- Kobozieff and Kobozieff, 1954; Yonamine et al., 1980). We did not observe any ossification centers in the anconeal process. In the oldest work it has been considered only by Hare in 1959 and by Chapman in 1965. Hare reported its appearance at 60 days of age in dogs from different non specified breeds (Hare, 1959b), while Chapman described its appearance at

45 days of age in Beagles (Chapman, 1965). In the last years, the presence of this center has been broadly investigated in large breeds (German Shepherd dog, Greyhound, Doberman Pinscher, Golden Retriever, Labrador Retriever mix and Pit Bull dog) in order to study elbow dysplasia (Breit et al., 2004; Cook and Cook, 2009; Cross and Chambers, 1997; Frazho et al., 2010; Gasch et al., 2012; Michelsen, 2013). Since there is a variability on the modality of appearance of this center (Frazho et al., 2010), its absence in small breeds dog should be further investigated, considering dogs older than those examined in this study

In 2/5 German Shepherd dogs observed by Hare, the distal epiphysis were formed by 2 ossification centers that fused rapidly to form the principle center. A similar behavior was observed for the proximal epiphysis in 1/5 dog of the same breed, however it was not specified which of the two principal ossification centers was involved. The same Author observed that the timing in ossification centers appearing and development was comparable in German Shepherd, Collie and Beagle dogs, while in Bulldog breed (just one dog) it developed later (Hare, 1961).

Regarding *carpus,* it is generally indicated that the center for the body of the accessory bone is the first that appears, successively appear the centers for the other carpal bones and finally appears the epiphysis of the accessory bone that appears from the 6^{th}-7^{th} week of age and elaborates the cap of the enlarged palmar end of the bone (Chapman, 1965; Pomriaskinsky- Kobozieff and Kobozieff, 1954; Ticer, 1984).

Os carpi accessorium showed a non homogeneous appearance, in fact it was not evident in group 1, it was not constant in groups 2 and 3, but it was evident in all the subjects of group 4. These observations are in agreement with Literature (Chapman, 1965a, b). Authors reported in fact that the center appears during the second and third week of age (Alvarado Morillo, 2007; Chapman, 1965; Hare, 1959b, 1961; Pomriaskinsky- Kobozieff and Kobozieff, 1954; Ticer,

1984). The epiphysis of the accessory bone wasn't radiographically evident in this study and these data agree with Literature (Chapman, 1965).

Regarding *os carpale intermedioradiale,* Evans and Miller reported that it derives from three different ossification centers which develops independently and fuses before birth (Evans and Miller, 2013). In this study, *os carpi radiale* and *os carpi intermedium* were evident starting from the fourth week of age, while *os carpi centrale* wasn't evident. So we can reasonably speculate that *os carpi radiale* and *os carpi intermedium* start together their ossification process, during the third week of age, while *os carpi centrale* develops later, confirming what previously reported in Literature and adding that in toy-dog breeds it develops after the 28th day of age.

Os carpi radiale appeared only in 50% of subjects of group 4. These data agree only with some of the papers (Chapman, 1965; Hare, 1959b; Ticer, 1984) and with data reported by Hare in German Shepherd Dog and in Collie (Hare, 1961). Other papers instead reported an earlier radiographic appearance of *os carpi radiale* (Alvarado Morillo, 2007; Pomriaskinsky- Kobozieff and Kobozieff, 1954), or a later appearance, like said Hare about Bulldog (38-45 days of age) and Beagle dogs (28-42 days of age) (Hare, 1961).

Os carpi intermedium appeared constantly on radiographs starting from the fourth week of age. These data agree with what reported by Hare in 1959 and Ticer (Hare, 1959b; Ticer, 1984). Other papers reported an earlier appearance, like Hare said about German Shepherd dog (10-15 days of age) (Hare, 1961), or a later appearance, like Hare reported in Bulldog (31-38 days of age), Chapman in Beagles (30 days of age) and Yonamine et al. in Beagles (60 days of age) (Chapman, 1965; Hare, 1961; Yonamine et al., 1980a).

Os carpi centrale wasn't evident in this study and these data agree with what reported by some Authors, such as Chapman, Yonamine et al., Ticer and Hare in Bulldog and Beagle dogs (Chapman, 1965; Hare, 1961; Ticer, 1984; Yonamine et al., 1980). Some Authors, contrariwise, reported the appearance of

this center since the third week of age, like Hare in German Shepherd Dog and Collie and Pomriaskinsky-Kobozieff and Kobozieff in German Shepherd and Cocker (Hare, 1959b, 1961; Pomriaskinsky- Kobozieff and Kobozieff, 1954).

Os carpi ulnare appeared constantly starting from the fourth week of age. These data agree with what reported by some Authors and by Hare in 1961 in German Shepherd dog and Collie (Chapman, 1965; Hare, 1959b, 1961; Pomriaskinsky-Kobozieff and Kobozieff, 1954; Ticer, 1984), while Hare in 1961 reported a later appearance in Bulldog (59-68 days of age) and Beagle dog (28-42 days of age)(Hare, 1961). Interestingly, we do not observed any features of hypertrophic processes of the chondrocytes, even in the oldest subjects.

Os carpale I, II, III, IV appeared only in one dog of group 2 and in 50% of the subjects of group 4. Literature is not homogeneous regarding these centers, but most of the Authors reported the appearance of the carpal bones during the third and the fourth week of age (Alvarado Morillo, 2007; Chapman, 1965; Hare, 1959b, 1961; Pomriaskinsky- Kobozieff and Kobozieff, 1954; Ticer, 1984; Yonamine et al., 1980). Only Hare described a later appearance of these centers in Bulldog (28-31 days of age) and Beagle dog (21-42 days of age)(Hare, 1961).

Os ischii and *os pubis* were present at birth, according to Literature. If *os ischii* ossification center was present in all the subjects evaluated, *os pubis* showed a less homogeneous appearance; it was not constant in groups 1 and 2, but present in all the subjects of groups 3 and 4., and regarding *os pubis* these data are quite different from the results of the study (Chapman, 1965b; Hare, 1960c, 1961; Smith, 1964; Ticer, 1984), even if according to other Authors *os pubis* appear until several weeks after birth in Beagle dog (Evans and Miller, 2013).

Os acetabulum, crista iliaca, tuber ischiadicum, arcus ischiadicus were not evident in this study and these data agree with what reported by previous Authors (Ticer, 1984).

Caput ossis femoris appeared in one subject in the second and one subject in the third group, and it was constant in group 4. These data don't agree completely

with Literature because according to most of the papers *caput ossis femoris* appear during the first or at least the second week of age (Chapman, 1965; Hare, 1960a, 1961; Ticer, 1984; Zoetis et al., 2003). Nevertheless, in group 4 the shape of *caput ossis femoris* becomes more hemispheric, resembling the final shape of the bony epiphysis.

Trochanter major and *trochanter minor* weren't radiographically evident in this study and these data agree with what reported by previous Authors (Bressou et al., 1957; Hare, 1960a, 1961);(Chapman, 1965; Fukuda and Matsuoka, 1980; Ticer, 1984; Zoetis et al., 2003).

Trochlea femoris appeared in in 50% the subjects of group 4. Regarding this ossification centers data from Literature are even more fragmentary, in fact only Ticer and Zoetis reported its appearance starting from 14 days of age (without specifying in which breeds), (Ticer, 1984; Zoetis et al., 2003). Therefore our data are quite different from what previously reported.

Condylus lateralis and *condylus medialis* appeared in one of the subjects of group 2 and in 50% the subjects of group 4. These data are in agreement with timing indicated by Zoetis et al. between 14 and 28 days of age (Zoetis et al., 2003), but they differ slightly from Ticer that indicated a more tardive appearance, starting from 21 days of age, (Ticer, 1984) . The subject 29, again, showed an early appearance of most of the *nuclei* observed both in the hind limb and forelimb.

Patella, wasn't evident in this study and these data agree with what reported by previous Authors. Timing of appearance of this small bone is rather variable, going from 30 days of age in German Shepherd dog (Hare, 1961) to 180 days of age in dogs of different breeds (Hare, 1960a).

The tibial proximal epiphysis appeared on radiographs in one subject of group 2 and in all the subjects of group 4. Only Fukuda and Matsuoka (Fukuda and Matsuoka, 1980) described the timing of appearance of this ossification center and they reported that it can occur at 30 days of age, so, in any case, the

appearance of this center is precocious if compared with the appearance in Beagle breed.

Cochlea tibiae appeared in one of the subjects of group 2 and in 50% of the subjects of group 4. Previous papers described the timing of appearance of this ossification center and they reported that the ossification center appear on radiographs between 11 and 31 days of age. Our data suggest that in toy breed could be a delay in the appearance of this center, considering the subjects of group 3 and 4 (Bressou et al., 1957; Chapman, 1965; Fukuda and Matsuoka, 1980; Hare, 1960a, 1961; Zoetis et al., 2003).

Tuberositas tibiae and *malleolus medialis* weren't evident in this study and these data agree with what reported by previous Authors (Bressou et al., 1957; Chapman, 1965; Fukuda and Matsuoka, 1980; Hare, 1960a, 1961; Ticer, 1984; Zoetis et al., 2003).

Calcaneus was evident in all the subjects of this study, excluding two subjects of group 2 and these data confirm the Literature, because *calcaneus* was present on radiographs at birth in all the breeds described (Bressou et al., 1957; Chapman, 1965; Fukuda and Matsuoka, 1980; Hare, 1960a, 1961; Ticer, 1984; Zoetis et al., 2003).

Talus became constant from the third week of age, while its appearance is less homogeneous in the first two weeks. These data disagree with Literature, like *calcaneus, talus* too is present at birth in all medium and large dog breeds considered (Bressou et al., 1957; Chapman, 1965; Fukuda and Matsuoka, 1980; Hare, 1960a, 1961; Ticer, 1984; Zoetis et al., 2003).

Os tarsi centrale appeared in 100% of the subjects of group 4, confirming data reported by Hare in 1960 (Hare, 1960a), again by Hare in 1961, in Beagle (Hare, 1961) and by Ticer (Ticer, 1984). Hare in 1961 reported that in Bulldog it appears between 31 and 38 days of age, while other papers (Bressou et al., 1957; Chapman, 1965) and Hare in German Shepherd and Collie (Hare, 1961)

described an earlier appearance (10-15 days of age in German Shepherd dog, 11-17 days of age in Collie).

Os tarsale III was evident on radiographs only in 50% of the subjects of group 4. These data agree with Bressou, Hare (only about German Shepherd dog, Collie and Beagle) and Ticer (Bressou et al., 1957; Hare, 1961; Ticer, 1984), while others Authors, and Hare in Bulldog, described a later appearance (Chapman: 30 days of age in Beagle, Hare: 31-38 days of age in Bulldog) (Chapman, 1965; Hare, 1960a).

Os tarsale IV was evident on radiographs in one subject in group 2, one in group 3 and in 100% of the subjects of group 4. These data disagree with data reported by previous Authors because they described an earlier appearance. Bressou in particular, described its appearance starting from 8-9 days of age in GSD, 9-10 days of age in Cocker, 13 days of age in Epagneul Breton, Chapman from 18 days of age in Beagle, Hare from 7-15 days of age in GSD, 7-17 in Collie, 11-21 in Beagle, Ticer from 14 days of age (Bressou et al., 1957; Chapman, 1965; Hare, 1960a, 1961; Ticer, 1984).

Os tarsale I and *II* weren't radiographically evident, according with Literature. Only Bressou, described the timing of appearance on radiographs of *os tarsale I* and *II*, at 26 or 25 days of age respectively, and so it can be assumed that they are not yet visible in this study (Bressou et al., 1957).

In conclusion, we can affirm that, generally, the samples examined showed an homogeneous behavior within the group. The appearance of most of the ossification centers reflects the timing of appearance of medium and large breed dogs, however the behavior of some ossification centers change and therefore might be considered as typical of toy-dog breeds.

Radiological analyses demonstrated that the time of appearance of the centers of ossification of the limbs was positively correlated with the age, though there

was some discrepancy. Morphological analyses confirmed these data and showed that, as expected, the grade of ossification inside the centers increased with growing age.

All the samples were well preserved and did not showed morphological alteration due to the process of freezing and thawing.

Endochondral ossification is the process by which the embryonic cartilaginous model of bones provides to their growth and is gradually replaced by bone. Morphological changes of the chondrocytes occur in the same orderly sequence both in primary and secondary centers of ossification (Mackie et al., 2011), but the expansion of the two centers is driven by a different spatial organization of these cells (Byers and Brown, 2006). First, chondrocytes undergo proliferation, which is observed also as the presence of pairs of chondrocytes in a single lacuna within the cartilage ECM. Round proliferative chondrocytes synthesize typical cartilage ECM components around themselves, in the form a columnar layer in the growth plate of the primary ossification center. In rabbit a growth plate has been described also during the formation of the secondary centers in long bones, but it is arranged around a noodles-like structure of hypertrophic cells encased in enlarged lacunae (Rivas and Shapiro, 2002). Chondrocytes gradually become hypertrophic, modeling their surrounding ECM as they expand, and then mineralizing and subsequently they undergo physiological death. Septa of the cartilage ECM surrounding them are partially removed, allowing entry of vessel and the mixture of cells responsible for the expansion of the ossification center (Amizuka et al., 2012). These processes occur in a different manner in primary and secondary ossification centers (Pazzaglia et al., 2011).

In our knowledge, this is the first work that describes the appearance and the morphological changes of the ossification centers in the epiphyses of limb bones of the dog during the first month of life. As expected, we observed that ossifications processes occur as in other species (Burkus et al., 1993) (Lefebvre and Bhattaram, 2010) and, as in rabbit, (Rivas and Shapiro, 2002) it possible to

categorize the progression of these events into groups. In rabbit, it was established that long bone and epiphyseal development progress through sixteen structural stages, starting from prenatal life (12 days old embryos) up to post natal life (18 month adult animal). We evaluated only the first month of life of the subjects, therefore we identified four structural stages of ossification. Interestingly, for OCT 1, 2 and 3 it was possible to establish with a rough degree of accuracy, a correlation between the pattern of organization at histological level and the radiographic aspect documented by x-rays during the time interval of single bone development, according with Pazzaglia (Pazzaglia et al., 2011). The presence of hypertrophic chondrocytes and enlarged lacunae (OCT1) indicated calcium salt deposition on the cartilage matrix between the cells and corresponded the first opacities in the middle of the cartilaginous epiphysis observed in the precocious phase of the ossification center. When the same assumed a rounded contour, it corresponded to the formation of a more structured center with calcified trabeculae and neo-formed bone tissue (OCT2-OCT3). Moreover, a further indication of the developmental change of the ossification center was its variation from a spherical form (OCT1-2) to hemispheric shape (OCT3), becoming more conformed to the final shape of the bony epiphysis. This was evident also in radiographic images, mainly in the proximal epiphysis of *humerus* and *femur*, as previously demonstrated by Yonamine et al. (Yonamine et al., 1980) in growing Beagles. The lack of correspondence between the morphological appearance of OCT0 and x-rays images, although in the presence of hypertrophic chondrocytes, might be to low levels of mineralization therefore indicating a very precocious stage of ossification. Most of the ossification centers of the forelimb was of type 2 and 3. At the moment we can only suppose that ossification processes were faster in these bones than in most of the bones of the hind limb, however our hypotheses must be confirmed on a more homogeneous and consistent number

of subjects and by focusing our studies also on the molecules and the mechanisms that drive the ossification of the bony limbs.

Interestingly, morphological analyses confirm the presence of two ossification centers in the proximal row of the carpus of the two subjects of the fourth group and that they were encased in a unique cartilaginous, corresponding to the intermedioradial bone. This is in agreement with the textbook*: "*Miller's anatomy of the dog" where it has been reported that during the fetal life, in the Beagle dog "each carpal element chondrifies independently, before loosing its identity, the intermediate carpal element fuses with the radial carpal bone and the two, in turn, fuse with the central element". Thus, by 42 days of gestation, if not before, there are only seven carpal cartilages, as in adult subjects (Evans and Miller, 2013).

Another innovative contribution of this work is the detection of morphometric parameters useful to evaluate the growth of the appendicular skeleton in toy-dog breeds in the first 28 days of life. There is in fact little research addressing morphometric measures of the canine skeleton and the relationship of these parameters and the biological age of the subjects.

In the dog, morphometry is routinely employed in the gestational age in order to date the birth through ultrasound (Beccaglia et al., 2008a; Beccaglia et al., 2008b; Beccaglia and Luvoni, 2006, 2012; Luvoni and Beccaglia, 2006). Only recently, a paper has been published regarding Miniature Pinscher breed dog and it provides morphological and morphometrical data dealing with 45-days-old *fetuses*, showing that they can be employed to evaluate the gestational age of the *fetuses* (de Oliveira Bezerra et al., 2013).

On adult dogs, most of the studies have been performed to establish breed standard of German Shepherd Dog and Cavalier King Charles Spaniel by measuring cranial diameters (Driver et al., 2010; Onar, 1999; Schmidt et al., 2011). Onar (Onar, 1999) in particular, showed that between 45 and 105 days

of age, the skull grows proportionally to the age of the subjects even if the neurocranium seems to grow more than the viscero-cranium. Onar and Gunes, in 2003, demonstrated that the length of the skull of German Shepherd puppies increased more than the width and, accordingly, the skull became narrower and longer with age (Onar and Gunes, 2003).

The skull of Cavalier King Charles Spaniel has been studied for his predisposition to Chiari-like malformation and syringomyelia (Schmidt et al., 2011). In this contest, Driver et al. (Driver et al., 2010) evaluated by Magnetic Resonance Imaging the skull of Cavalier King Charles Spaniel dogs, with less than 2 years of age and with symptoms consistent with syringomyelia, and the skull of dogs of the same breed with more than 5 years of age presenting central nervous system symptoms without syringomyelia. The Authors measured and compared brain parenchyma with ventricular system volume and they showed that in the Cavalier King Charles Spaniel breed, like in human being, the overcrowding of the posterior fossa is quite common, due to abnormal skull conformation which predisposes to the onset of syringomyelia.

Radiological morphometry has been employed to evaluate canine hip joint through the dorsal acetabular rim view and the center-edge angle (Meomartino et al., 2002). Authors performed a prospective comparison with the center-edge angle (CE) and the acetabular slope angle (AS) to evaluate the acetabular coverage of the femoral head in the dorsal acetabular rim view in a huge number (208) of hip joints of large and giant breed dogs. They concluded that the CE angle is more reliable than the AS angle and that the dorsal acetabular rim view gives valuable data in the early stages of canine hip dysplasia. In 2006, Osmond et al. performed a morphometric assessment of the proximal tibia in dogs with and without cranial cruciate ligament rupture. They concluded that the characterization of the shape of the proximal portion of the tibia contributes to understand the pathogenesis of steep tibial plateau slope and helps in optimizing the surgical management of dogs with cranial cruciate ligament rupture

(Osmond et al., 2006). According with these results, three years later, Mostafa et al. (Mostafa et al., 2009) through radiographic and tomographic examination demonstrated that in Labrador Retrievers the cranial angulation of the proximal portion of the tibia, excessive steepness of the tibial plateau and, in addition, distal femoral torsion appeared more likely to be associated with CCL deficiency than femoral angulation, tibial torsion, intercondylar notch stenosis, and increased inclination of the patellar ligament. In 2010, other Authors assess the canine hip joint using morphometric evaluation of the acetabular angle of retrotorsion. They tried to compare the acetabular angle of retrotorsion (AAR) with the Norberg angle (NA) and the hip score (HS) in 387 Leonberger dogs and to determine the AAR cut off value in order to differentiate between normal and dysplastic dogs. They concluded that AAR can be considered a reliable morphometric assessment tool in evaluating the acetabular conformation and the grade of hip dysplasia (Doskarova et al., 2010).

To our knowledge, there are only two papers regarding morphometric studies of the skeletal development in dogs. As expected, they were carried out on Beagle dogs (Delaquerriere-Richardson et al., 1982; Helmsmuller et al., 2013). In the first study Authors performed a correlation between age, body weight, x-ray morphometrical measurements and x-ray photodensitometry of the bones of standardized colony-raised male research Beagles of 13 and 21 months. They showed that the total width of *os femoris* and its optical density increased significantly with age and body weight (Delaquerriere-Richardson et al., 1982). Interestingly, morphometric analyses carried out through Magnetic Resonance Imaging showed that femoral measurements can be employed to evaluate and describe fetuses development and growth (Connolly et al., 2004).

The second study on the dog is a quite extended paper regarding the ontogenetic allometry of the Beagle. Authors monitored the ontogenetic development of 6 Beagle between 9 and 51 weeks of age to investigate their skeletal allometry and compare these results with data from others lines, breeds and species. Statistical

analysis showed that withers and pelvic height and trunk length have positive allometry compared to body mass. Coefficients of segment lengths to body mass exhibited positive allometry for *scapula*, *brachium, antebrachium, femur* and *crus*. They concluded that a puppy's size at 9 weeks is a good indicator for its final size, although only male siblings were investigated and no considerations regarding sex related differences could be drawn. Among siblings, growth duration may vary substantially and seems to be not related with the adult size, while within breeds, they hypothesized a longer time to reach maturation for larger breed dogs, and finally, potential factors which can be responsible for variations in the ontogenetic allometry of the mammals need further investigations (Helmsmuller et al., 2013).

In our study, we demonstrated that in toy-dog breeds, categorized in a unique group depending on their body weight, there was a very strong correlation between the radiographic measures themselves and body mass and age. Moreover, age showed the highest correlation with cranial length. Weight showed the highest positive correlation with crown-rump length. Diaphyseal lengths, included femoral length, were highly and positively correlated between them, with age and with skull and cranial lengths. High positive correlations were also evident between cranial length and neurocranium width, between zigomatic width and both vertebral column length and crown-rump length.

Correlations involving viscero-cranial lengths were no significant or showed lower level of correlation if compared with those described before. First of all, these data may be due to the different skull conformation of the subjects enrolled in the study, in fact the differences between brachycephalic, mesaticephalic and dolichocephalic breeds were not considered in this work (Evans and Miller, 2013). Moreover, in breeds with a "more rounded" skull, like Chihuahua, it is important to consider also the inherent difficulties in measuring viscero-cranial length, because, in the radiographic projections taken

into consideration, it was quite difficult to identify the junction on the median plane of the right and left nasofrontal sutures.

Therefore we can conclude that femoral length could be taken into consideration as a parameter to assess the developmental rate and the age of toy-dog breeds during the growing period, particularly in the first 4 weeks of age. Excluding evaluation involving viscero-cranial length, also skull and cranial measurements could be reasonably employed to evaluate these breeds.

We generally observed strong correlations also between radiographic measurements and the measurements of the corresponding anatomical compartment for long bones, body and skull measures. Moreover, within anatomical measures, significance levels were the same described for radiographic valuations. Interestingly, the most significant correlations observed were between neurocranium width and bones lengths, included femoral length. As for radiographic observations, most of the less significant correlations involved skull length, and subsequently viscero-cranial lengths. Other less significant correlations involved crown-rump length and vertebral-column length. These data may be due to the difficult to find, on the cadavers, the exact landmarks to perform the measurements. As consequence, it is possible that measures were not precise. A low level of correlation was also described between radial length and age. As previously, the identification of the landmarks of these bone was not always manageable because radius is not the only skeletal basis of the forearm and the landmarks of the radial proximal epiphysis on the cadavers were difficult to achieve through the caliber due to the anatomical conformation of the elbow joint.

To better evaluate as skeletal limbs develop during the first month of life in toy-dog breeds we correlated ossification centers appearance and long bones length.

In our knowledge, there are no previous papers, which described these correlations. Statistical analysis showed strong significance between the radiographic appearance of humeral proximal epiphysis and humeral length, of *corpus ossis accessori* and both radial and ulnar lengths, of *os pubis* and femoral length, of *caput ossis femoris* and femoral length, of *talus* and femoral and tibial lengths and between *os tarsale IV* and tibial length.
Since most of the correlations between ossification centers appearance and long bone measurements were highly significant, we could assume that long bone length is indicative for the presence of specified ossification centers, and indirectly that long bone measurement could have an important role in estimation of the age of growing puppies.

To our knowledge, no densitometric study was performed to evaluate the ossification in newborn toy-dog breeds and no correlation between bone mineral density (BMD) and long bones length is present in literature. Dual-energy X-ray absorptiometry is "one of the most reliable densitometric technique for spatial resolution, precision and accuracy and it allows the analysis of small specimens" to evaluate bone density (Panattoni et al., 1999). Therefore, it is important to perform accurate positioning to prevent inadvertent alteration of bone mineral density as demonstrated in a previously study performed on *humerus, radius, os femoris* and *tibia* from adult dogs (Markel et al., 1994).
In Medicine, there are different papers regarding the application of DXA to measure bone mineral density in newborns and infants to evaluate skeletal development and biological age (Braillon et al., 1992; Brunton et al., 1993; Salle et al., 1992; Tsukahara et al., 1993). Panattoni et al.(Panattoni et al., 1999) performed a densitometric analysis to study the ossification of human fetal skeleton in relation to conceptual age. They observed that in human fetal skeleton, BMD is progressively less correlated with conceptual age and suggest an individual variability in bone density at term of development and particularly

at the level of spongiosa, of proximal and distal end of the bone, the areas mostly involved in architectural changes during the morphogenesis of the long bones (Panattoni et al., 1999). With the same technical approach and on they same samples, they observed a different timing in the appearance of lesser and greater trochanter (Panattoni et al., 2000). Recently other Authors presented a review regarding considerations and correlations between bone growth, bone calcium accretion and bone mineral density. They concluded that endochondral bone growth and bone elongation, in a subregion of the spongiosa, are associated with bone calcium accretion, and this accretion leads to an increase in BMD. Endochondral bone growth and bone elongation don't determine peak bone mass, which is probably predetermined by genetic factors, but endochondral bone growth could determine the size of the skeletal framework (Wongdee et al., 2012).

In dog, dual-energy x-ray absorptiometry has been used to measure bone mineral density of healed femora after fracture fixation with a leg-lengthening plate. In this context, Muir el al. demonstrated that clinically apparent lameness of three of their patients did not constantly appear to be associated with altered bone mineral density and it may have been caused by hip osteoarthritis, by screw loosening or by a non displaced diaphyseal fracture, associated with extensive post-traumatic soft tissue injury (Muir et al., 1995).

In this study, it was calculated the general BMD of the diaphysis of *radius* and *ulna*, and *femur*. Due the small size of the specimens, it would have been difficult to choice accurately a precise area in the metaphysis and another one in the diaphysis in order to investigate the progression of the ossification in the different parts of the bones and to describe possible differences in BMD as others authors previously reported in human being (Panattoni et al., 2000; Panattoni et al., 1999), and so it was calculated only the general BMD of the diaphysis of *radius* and *ulna*, and *femur*.

The BMD analysis of *radius* and *ulna*, and *os femoris* showed that general BMD of these bones increases increasing the age of the subjects and that these bones show a similar trend and behave in the same way. The minimum value of BMD of *radius* and *ulna* and of *os femoris* was detected in the youngest subject (subject n.1), and the maximum value of BMD of *radius* and *ulna* and of *os femoris* was detected in the oldest subject (subjects n. 35). The mean values of the 4 groups of the different BMD detected show, in general, an increasing trend of the BMD during the time. Moreover, Sperman bivariate correlation showed high significance between the general bone mineral density of *radius* and *ulna* and both radial and ulnar lengths, and between the general bone mineral density of *os femoris* and femoral length. These data confirm that increasing BMD is highly correlated with increasing long bones length and seem to confirm the spatio-temporal relationship between BMD in canine newborn skeleton and in long bones growth. Furthermore, long bone growth and BMD, representing indirectly endochondral bone growth and bone calcium accretion, confirm what previously reported in rats (Wongdee et al., 2012), that these parameters should in general show positive correlation.

Only four subjects (n. 26, 27, 29, 35) showed some differences regarding ossification centers appearance or BMD.

Subjects n. 26, 27 and 35 in particular, showed a later appearance of most of the ossification centers, while subject n. 29, showed an early appearance of most of the ossification center, both in the hind limb and forelimb.

The role of weight in the appearance of ossification center is unclear. A positive correlation between weight and skeletal development at birth was not demonstrated (Helmsmuller et al., 2013). According with the Authors, we observed that, although this subject (n. 29) had elevated body weight if compared with the subjects of the same group, morphometric radiological and

anatomical measures did not influence the mean values of the groups. Therefore, we supposed that this peculiar behavior could be due to a highest skeletal maturity level due to individual and/or breed variability.

Conversely, dogs number 26, 27 and 35 showed a delayed development respect to group where they were enrolled. This "immaturity" could be explained with an individual difference, but dogs number 26 and 27 were brothers, and we cannot exclude the possibility of a premature day of birth. Pregnancy lifetime and nutritional factors could have an important role in the variability of the sample and in the growth rate (Eilts et al., 2005; Lopate, 2008). The first days of life in fact are the results of the interaction between fetal genotype and uterine environment and especially of the size of *uterus*, mostly in the last days of pregnancy. In human being and mice, as well as in dog, it was observed that the puppies born in larger litters have lower weight than those born in smaller litters (Vanden Berg-Foels et al., 2006). In Labrador breed a negative association was also detected between birth weight and age, regarding the ossification of the femoral head, and it would seem imputable to skeletal maturity of subjects rather than to their body weight (Vanden Berg-Foels et al., 2006). However, it is interesting to note that the differences due to body weight decreased with the increasing of age, and in Labrador breed dogs these differences are already reduced at 8 days after birth and they're no more detectable at 12 days after birth.

Therefore, if we do not take in account subjects 26 e 27 e 29, e 35 we can conclude that generally, *calcaneus* was present at birth confirming what reported Literature for medium and big size dogs while *talus* and *os pubis* appears only two weeks later.

Timing of appearance of *humeral proximal epiphysis, trochlea radii,* most of *ossa carpi*, *trochanter major* and *trochanter minor os femoris, tibial proximal epiphysis* and *os tarsi centrale* was comparable with the timing described in large breed dogs.

Caput radii, the distal epiphysis of *humerus* and of *os femoris,* and *caput ossis femoris* show a non homogeneous behavior compared to the timing described in large breed dogs, since they were present only in a small number of subjects due to the sample size of group 4.
Due to the lack of information of the Literature and to the non homogeneus behavior of these ossification centers in our study, we cannot perform a evaluation regarding the timing of these centers.

Statistical analysis showed no significance between the appearance of *calcaneus* and femoral and tibial length. According to Literature, *calcaneus* is radiographically evident at birth, but in this study, again in subject n.26 and 27, it was not evident, and so these data could have turned away the statistical results from the expectations, and it could be reasonably assumed that excluding this subjects even the correlations between the appearance of *calcaneus* and femoral and tibial length would have shown high significance as the others.

The mean values of BMD of subject n. 29 are higher than BMD values of the other subjects of the same group and even of the subjects of group 3. As previously reported, the peculiarity of this subject was an elevated body weight. It has been demonstrated that a greater height and body mass index (BMI) gain in prenatal life and infancy are associated to higher peak bone mass, and greater BMI gain in childhood/adolescence are associated to higher peak BMD (Tandon et al., 2012). Moreover, even if endochondral bone growth is the first mechanism that influences bone morphology and bone mineral accretion, nutritional status or patho/physiological conditions or physical activity can impact bone microstructure and calcium accumulation (Wongdee et al., 2012). Conversely, other Authors, in a study on growing Beagle, reported that the lightest dog did not reach its adult mass before the heaviest and *vice versa* (Helmsmuller et al., 2013). A different skeletal maturity level due to individual

and/or breed variability rather than to body weight *per se* must always be considered.

Finally, sex did not seem to influence the appearance of ossification center and skeletal development in toy-dog breeds within 28 days of age. Generally, toy dog breeds do not show great difference in size between male and female. However, even if it should happen, it is possible that these differences will arise later in time. Moreover, previous studies showed significant ontogenetic differences between sexes only for large breeds, but not for smaller breeds (Helmsmuller et al., 2013; Yonamine et al., 1980a).

Conclusion

This work describes and characterizes, for the first time, skeletal growth and development of newborn toy-dog breeds. Radiographic and histological evaluation of the appearance of the ossification centers of the limbs, morphometric evaluation of skull, limbs and vertebral column, and bone mineral density of limb bones provided practical indications to estimate the age and the skeletal of growing puppies of these breeds.

From this point of view, during the first month of life, newborn toy-dog breeds can be considered as a homogeneous population. We could assume that long bone length is indicative for the presence of specified ossification centers and that long bone measurement could have an important role to assess the developmental rate and the age of toy-dog breeds during the growing period, particularly in the first 4 weeks of age. Skull, cranial and long bone lengths can be reasonably employed to evaluate these breeds by X-rays analysis, while the anatomical measurements of humeral, femoral and tibial lengths as well as neurocranium width could replace the radiographic measure of the corresponding skeletal segment in order to assess the growth of toy-breed dogs during the first month of life without exposition to ionizing radiation.

The densitometric analysis shows an increasing trend between BMD of *radius, ulna* and *os femoris* and it presents a significant correlation with age and long bones growth in the first month of life in new-born toy breed dogs and it could reasonably consider a valid tool in evaluation of skeletal development in growing puppies.

Finally, further studies must be undertaken in order to improve the sample size, even if these results already take particular relevance because it must be considered that the study has not been carried out on the basis of an experimental model and only subjects died for unrelated reasons with the study were enrolled.

Bibliography

Authors Committee, 2012, Nomina Anatomica Veterinaria, 5th edition, v. 1, 160 p.

Alpak, H., R. Mutus, and V. Onar, 2004, Correlation analysis of the skull and long bone measurements of the dog: Ann Anat, v. 186, p. 323-30.

Alvarado Morillo, M., 2007, Age Determination in young Keeshound Puppies Using a simple Radiographic Study of Radius, Ulna and Carpus: Multiciencias, v. 7, p. 249-255.

Amizuka, N., T. Hasegawa, K. Oda, P. H. Luiz de Freitas, K. Hoshi, M. Li, and H. Ozawa, 2012, Histology of epiphyseal cartilage calcification and endochondral ossification: Frontiers in Bioscience, v. 4, p. 2085-100.

Beccaglia, M., P. Anastasi, E. Grimaldi, A. Rota, M. Faustini, and G. C. Luvoni, 2008a, Accuracy of the prediction of parturition date through ultrasonographic measurement of fetal parameters in the queen: Vet Res Commun, v. 32 Suppl 1, p. S99-101.

Beccaglia, M., M. Faustini, and G. C. Luvoni, 2008b, Ultrasonographic study of deep portion of diencephalo-telencephalic vesicle for the determination of gestational age of the canine foetus: Reprod Domest Anim, v. 43, p. 367-70.

Beccaglia, M., and G. C. Luvoni, 2006, Comparison of the accuracy of two ultrasonographic measurements in predicting the parturition date in the bitch: J Small Anim Pract, v. 47, p. 670-3.

Beccaglia, M., and G. C. Luvoni, 2012, Prediction of parturition in dogs and cats: accuracy at different gestational ages: Reprod Domest Anim, v. 47 Suppl 6, p. 194-6.

Boulay, J. P., 1998, Fragmented medial coronoid process of the ulna in the dog: Veterinary Clinics of North America-Small Animal Practice, v. 28, p. 51-+.

Boyne, M. S., M. Thame, C. Osmond, R. A. Fraser, L. Gabay, M. Reid, and T. E. Forrester, 2010, Growth, body composition, and the onset of puberty: longitudinal observations in Afro-Caribbean children: J Clin Endocrinol Metab, v. 95, p. 3194-200.

Braillon, P. M., B. L. Salle, J. Brunet, F. H. Glorieux, P. D. Delmas, and P. J. Meunier, 1992, Dual energy x-ray absorptiometry measurement of bone mineral content in newborns: validation of the technique: Pediatr Res, v. 32, p. 77-80.

Breit, S., W. Kunzel, and S. Seiler, 2004, Variation in the ossification process of the anconeal and medial coronoid processes of the canine ulna: Res Vet Sci, v. 77, p. 9-16.

Bressou, C., N. Pomriaskinsky-Kobozieff, and N. Kobozieff, 1957, Étude radiologique de l'ossiffication du squelette du pied du Chien aux divers stade de son évolution, de la naissance à l'âge adulte, *in* V. Freres, ed., Recueil de Médecine Vétérinaire, v. Tome CXXXII.

Brianza, S. Z. M., M. Delise, M. M. Ferraris, P. D'Amelio, and P. Botti, 2006, Cross-sectional geometrical properties of distal radius and ulna in large, medium and toy breed dogs: Journal of Biomechanics, v. 39, p. 302-311.

Brunton, J. A., H. S. Bayley, and S. A. Atkinson, 1993, Validation and application of dual-energy x-ray absorptiometry to measure bone mass and body composition in small infants: Am J Clin Nutr, v. 58, p. 839-45.

Burger, I. H., 1994, Energy needs of companion animals: matching food intakes to requirements throughout the life cycle: The Journal of nutrition, v. 124, p. 2584S-2593S.

Burk, R., and D. A. Feeney, 1996, Small Animal Radiology and Ultrasound: A Diagnostic Atlas and Text, Saunders.

Burkus, J. K., T. M. Ganey, and J. A. Ogden, 1993, Development of the cartilage canals and the secondary center of ossification in the distal chondroepiphysis of the prenatal human femur: The Yale journal of biology and medicine, v. 66, p. 193-202.

Burton, N. J., M. J. Perry, N. Fitzpatrick, and M. R. Owen, 2010, Comparison of bone mineral density in medial coronoid processes of dogs with and without medial coronoid process fragmentation: American Journal of Veterinary Research, v. 71, p. 41-6.

Byers, P. D., and R. A. Brown, 2006, Cell columns in articular cartilage physes questioned: a review: Osteoarthritis and cartilage / OARS, Osteoarthritis Research Society, v. 14, p. 3-12.

Carlson, W. D., 1967, Veterinary Radiology: Philadelphia, Lea & Febiger.
Carrera, I., G. J. C. Hammond, and M. Sullivan, 2008, Computed tomographic features of incomplete ossification of the canine humeral condyle: Veterinary Surgery, v. 37, p. 226-231.
Castillo, R. F., and C. Ruiz Mdel, 2011, Assessment of age and sex by means of DXA bone densitometry: application in forensic anthropology: Forensic science international, v. 209, p. 53-8.
Chapman, W., 1965, Appearance of ossification centers and epiphyseal closures as determined by radiographic techniques: J Am Vet Med Assoc, v. 147, p. 138-141.
Charjan, R. Y., V. R. Bhamburkar, S. B. Banubakode, R. S. Dalvi, N. C. Nandeswar, and V. H. Kadukar, 2002, Radiographic study on status of developing canine pectoral limb bones: Indian Journal of Veterinary Anatomy, v. 14, p. 43-50.
Connolly, S. A., D. Jaramillo, J. K. Hong, and F. Shapiro, 2004, Skeletal development in fetal pig specimens: MR imaging of femur with histologic comparison: Radiology, v. 233, p. 505-14.
Conzemius, M. G., G. K. Smith, C. T. Brighton, M. J. Marion, and T. P. Gregor, 1994, Analysis of physeal growth in dogs, using biplanar radiography: Am J Vet Res, v. 55, p. 22-7.
Cook, C. R., and J. L. Cook, 2009, Diagnostic imaging of canine elbow dysplasia: a review: Vet Surg, v. 38, p. 144-53.
Cross, A. R., and J. N. Chambers, 1997, Ununited anconeal process of the canine elbow: Compendium on Continuing Education for the Practicing Veterinarian, v. 19, p. 349-&.
Cunha, E., E. Baccino, L. Martrille, F. Ramsthaler, J. Prieto, Y. Schuliar, N. Lynnerup, and C. Cattaneo, 2009, The problem of aging human remains and living individuals: a review: Forensic Sci Int, v. 193, p. 1-13.
De Lahunta, A., and E. Habel, 1986, Applied Veterinary Anatomy: Philadelphia, W B Saunders Co.
de Oliveira Bezerra, D., H. de Barros Fernandes, A. Mendes Conte Junior, and L. de oliveira Lopes, 2013, External morphology and morphometry of canine fetuses of the pinscher breed to 45 days of post-coitus: Ciencias Agrarias, v. 34, p. 335-340.
Delaquerriere-Richardson, L., C. Anderson, U. M. Jorch, and M. Cook, 1982, Radiographic morphometry and radiographic photodensitometry of the femur in the Beagle at 13 and 21 months: American Journal of Veterinary Research, v. 43, p. 2255-2258.
Dennis, R., R. M. Kirberger, F. Barr, and R. H. Wrigley, 2010, Handbook of small animal radiology and ultrasound Techniques and differential diagnoses, Sauders.
Doskarova, B., M. Kyllar, and V. Paral, 2010, Morphometric assessment of the canine hip joint using the acetabular angle of retrotorsion: Vet Comp Orthop Traumatol, v. 23, p. 326-31.
Driver, C. J., C. Rusbridge, I. M. McGonnell, and H. A. Volk, 2010, Morphometric assessment of cranial volumes in age-matched Cavalier King Charles spaniels with and without syringomyelia: Vet Rec, v. 167, p. 978-9.
Dyce, K. M., W. O. Sack, and C. J. G. Wensing, 2010, Textbook of Veterinary Anatomy: St Louis-Missouri, Sunders Elsevier.
Eilts, B. E., A. P. Davidson, G. Hosgood, D. L. Paccamonti, and D. G. Baker, 2005, Factors affecting gestation duration in the bitch: Theriogenology, v. 64, p. 242-51.
Ellenberger, W., and B. Hermann, 1943, Handbuch der vergleichenden Anatomie der Haustiere: Berlin, Hirschwald, A., 1070 p.
Elmaz, O., O. A. Aksoy, A. Zonturlu, and S. Dikmen, 2008, The determination of growth performance and some morphological characteristics effective on development curves of German Shepherd puppies during the suckling period: Polish Journal of Veterinary Sciences, v. 11, p. 367-370.
Emmerson, T. D., T. J. Lawes, A. E. Goodship, C. Rueux-Mason, and P. Muir, 2000, Dual-energy X-ray absorptiometry measurement of bone-mineral density in the distal aspect of the limbs in racing Greyhounds: American Journal of Veterinary Research, v. 61, p. 1214-9.
Evans, H. E., and M. E. Miller, 2013, Miller's anatomy of the dog, xix, 850 pages p.
Franklin, D., 2010, Forensic age estimation in human skeletal remains: current concepts and future directions: Leg Med (Tokyo), v. 12, p. 1-7.

Frazho, J. K., J. Graham, J. N. Peck, and J. J. De Haan, 2010, Radiographic evaluation of the anconeal process in skeletally immature dogs: Vet Surg, v. 39, p. 829-32.
Fries, C. L., and A. M. Remedios, 1995, The Pathogenesis and Diagnosis of Canine Hip-Dysplasia - a Review: Canadian Veterinary Journal-Revue Veterinaire Canadienne, v. 36, p. 494-502.
Fujiki, M., Y. Kurima, K. Yamanokuchi, K. Misumi, and H. Sakamoto, 2007, Computed tomographic evaluation of growth-related changes in the hip joints of young dogs: Am J Vet Res, v. 68, p. 730-4.
Fukuda, S., and O. Matsuoka, 1980, Comparative studies on maturation process of secondary ossification centers of long bones in the mouse, rat, dog and monkey: Jikken Dobutsu, v. 29, p. 317-26.
Garmel, S. H., and M. E. D'Alton, 1994, Diagnostic ultrasound in pregnancy: an overview: Semin Perinatol, v. 18, p. 117-32.
Gasch, E. G., J. J. Labruyere, and J. F. Bardet, 2012, Computed tomography of ununited anconeal process in the dog: Vet Comp Orthop Traumatol, v. 25, p. 498-505.
Greulich, W. W., and S. Idell Pyle, eds., 1975, Radiographic Atlas of Skeletal Development of the Hand and Wrist, v. 1, Standford University Press.
Gustaffson, P. O., S. E. Olsson, H. Kasstrom, and B. Wennman, 1975, Skeletal development of greyhounds, German Shepherd dogs and their crossbreed offspring: Acta Radiologica, p. 81-107.
Hare, W. C., 1959a, Radiographic Anatomy of the Canine Pectoral Limb. Part I. Fully Developed Limb: J Am Vet Med Assoc, v. 135, p. 264-271.
Hare, W. C., 1959b, Radiographic Anatomy of the Canine Pectoral Limb. Part II. Developing Limb: J Am Vet Med Assoc, v. 135, p. 305-310.
Hare, W. C., 1960, Radiographic Anatomy of the Canine Pelvic Limb. Part II. Developing Limb: J Am Vet Med Assoc, v. 136, p. 603-601.
Hare, W. C., 1960, Radiographic Anatomy of the Canine Pelvic Limb. Part I. Fully developed limb: J Am Vet Med Assoc, v. 136, p. 542-549.
Hare, W. C., 1960, The age at which epyphiseal union takes places in the limb bones of the dog: Wien.tierarztl.Mschr.Festschrift Schreiber, v. 9, p. 224-225.
Hare, W. C., 1961, The ages at which the centers of ossification appear roentgenographically in the limb bones of the dog: Am J Vet Res, v. 22, p. 825-35.
Hawthorne, A. J., D. Booles, P. A. Nugent, G. Gettinby, and J. Wilkinson, 2004, Body-weight changes during growth in puppies of different breeds: The Journal of nutrition, v. 134, p. 2027S-2030S.
Hedhammar, A., L. Krook, and B. E. Sheffy, 1974a, Overnutrition and skeletal disease. An experimental study in growing Great Dane dogs. 3. Food consumption and weight gains: Cornell Vet, v. 64, p. Suppl 5:23-31.
Hedhammar, A., F. M. Wu, L. Krook, H. F. Schryver, A. De Lahunta, J. P. Whalen, F. A. Kallfelz, E. A. Nunez, H. F. Hintz, B. E. Sheffy, and G. D. Ryan, 1974b, Overnutrition and skeletal disease. An experimental study in growing Great Dane dogs: Cornell Vet, v. 64, p. Suppl 5:5-160.
Helmsmuller, D., P. Wefstaedt, I. Nolte, and N. Schilling, 2013, Ontogenetic allometry of the Beagle: BMC Veterinary Research, v. 9, p. 10 October 2013.
Isola, M., A. Zotti, P. Carnier, E. Baroni, and R. Busetto, 2005, Dual-energy X-ray absorptiometry in canine legg-Calve-Perthes disease: Journal of veterinary medicine. A, Physiology, pathology, clinical medicine, v. 52, p. 407-10.
Kealy, J. K., 1987, Diagnostic Radiology of the Dog and Cat, W.B. Saunders.
Kilborn, S. H., G. Trudel, and H. Uhthoff, 2002, Review of growth plate closure compared with age at sexual maturity and lifespan in laboratory animals: Contemporary Topics in Laboratory Animal Science, v. 41, p. 21-26.

Kutzler, M. A., A. E. Yeager, H. O. Mohammed, and V. N. Meyers-Wallen, 2003, Accuracy of canine parturition date prediction using fetal measurements obtained by ultrasonography: Theriogenology, v. 60, p. 1309-17.
Lefebvre, V., and P. Bhattaram, 2010, Vertebrate skeletogenesis: Current topics in developmental biology, v. 90, p. 291-317.
Lesbre, F. X., 1897, Contribution a l'etude de l'ossification du Squelette des Mammiferes Domestiques: Ann. Soc. Agri. Lyon, v. 7, p. 1-106.
Long, F., and D. M. Ornitz, 2013, Development of the endochondral skeleton: Cold Spring Harbor perspectives in biology, v. 5, p. a008334.
Lopate, C., 2008, Estimation of gestational age and assessment of canine fetal maturation using radiology and ultrasonography: a review: Theriogenology, v. 70, p. 397-402.
Luvoni, G. C., and M. Beccaglia, 2006, The prediction of parturition date in canine pregnancy: Reprod Domest Anim, v. 41, p. 27-32.
Mackie, E. J., L. Tatarczuch, and M. Mirams, 2011, The skeleton: a multi-functional complex organ: the growth plate chondrocyte and endochondral ossification: The Journal of endocrinology, v. 211, p. 109-21.
Madsen, J. S., I. Reimann, and E. Svalastoga, 1991, Delayed ossification of the femoral head in dogs with hip dysplasia: Journal of Small Animal Practice, v. 32, p. 351-354.
Mahler, S., and T. Havet, 1999b, Secondary ossification centre at the acetabular dorsal rim in a dog: radiographic and MRI observations: Revue de Medecine Veterinaire, v. 150, p. 433-440.
Marcellin-Little, D. J., D. J. DeYoung, K. K. Ferris, and C. M. Berry, 1994, Incomplete ossification of the humeral condyle in Spaniels: Veterinary Surgery, v. 23, p. 475-487.
Markel, M. D., E. Sielman, and J. J. Bodganske, 1994, Densitometric properties of long bones in dogs, as determined by use of dual-energy x-ray absorptiometry: American Journal of Veterinary Research, v. 55, p. 1750-6.
Markel, M. D., M. A. Wikenheiser, R. L. Morin, D. G. Lewallen, and E. Y. Chao, 1990, Quantification of bone healing. Comparison of QCT, SPA, MRI, and DEXA in dog osteotomies: Acta Orthop Scand, v. 61, p. 487-98.
Martin, R. B., L. Crews, T. Saveraid, and M. G. Conzemius, 2010, Prevalence of incomplete ossification of the humeral condyle in the limb opposite humeral condylar fracture: 14 dogs: Vet Comp Orthop Traumatol, v. 23, p. 168-72.
Meomartino, L., G. Fatone, A. Potena, and A. Brunetti, 2002, Morphometric assessment of the canine hip joint using the dorsal acetabular rim view and the centre-edge angle: J Small Anim Pract, v. 43, p. 2-6.
Michelsen, J., 2013, Canine elbow dysplasia: aetiopathogenesis and current treatment recommendations: Vet J, v. 196, p. 12-9.
Mostafa, A. A., D. J. Griffon, M. W. Thomas, and P. D. Constable, 2008, Proximodistal alignment of the canine patella: radiographic evaluation and association with medial and lateral patellar luxation: Veterinary surgery : VS, v. 37, p. 201-11.
Mostafa, A. A., D. J. Griffon, M. W. Thomas, and P. D. Constable, 2009, Morphometric characteristics of the pelvic limbs of Labrador Retrievers with and without cranial cruciate ligament deficiency: Am J Vet Res, v. 70, p. 498-507.
Muir, P., M. D. Markel, J. J. Bogdanske, and K. A. Johnson, 1995, Dual-energy x-ray absorptiometry and force-plate analysis of gait in dogs with healed femora after leg-lengthening plate fixation: Veterinary surgery : VS, v. 24, p. 15-24.
Nemec, U., S. F. Nemec, M. Weber, P. C. Brugger, G. Kasprian, D. Bettelheim, D. L. Rimoin, R. S. Lachman, G. Malinger, and D. Prayer, 2013, Human long bone development in vivo: analysis of the distal femoral epimetaphysis on MR images of fetuses: Radiology, v. 267, p. 570-80.
Newton, C. D., 1985, Textbook of Small Animal Orthopaedics: Ithaca, New York, USA., International Veterinary Information Service (www.ivis.org).

Nowlan, N. C., J. Sharpe, K. A. Roddy, P. J. Prendergast, and P. Murphy, 2010, Mechanobiology of embryonic skeletal development: Insights from animal models: Birth defects research. Part C, Embryo today : reviews, v. 90, p. 203-13.
Onar, V., 1999, A morphometric study on the skull of the German shepherd dog (Alsatian): Anat Histol Embryol, v. 28, p. 253-6.
Onar, V., and H. Gunes, 2003, On the variability of skull shape in German shepherd (Alsatian) puppies: Anatomical Record Part a-Discoveries in Molecular Cellular and Evolutionary Biology, v. 272A, p. 460-466.
Osmond, C. S., D. J. Marcellin-Little, O. L. Harrysson, and L. B. Kidd, 2006, Morphometric assessment of the proximal portion of the tibia in dogs with and without cranial cruciate ligament rupture: Vet Radiol Ultrasound, v. 47, p. 136-41.
Ozaki, S., K. Toida, M. Suzuki, Y. Nakamura, N. Ohno, T. Ohashi, M. Nakayama, Y. Hamajima, A. Inagaki, K. Kitaoka, H. Sei, and S. Murakami, 2010, Impaired olfactory function in mice with allergic rhinitis: Auris, nasus, larynx, v. 37, p. 575-83.
Panattoni, G. L., P. D'Amelio, M. Di Stefano, and G. C. Isaia, 2000, Ossification centers of human femur: Calcified Tissue International, v. 66, p. 255-8.
Panattoni, G. L., P. D'Amelio, M. Di Stefano, A. Sciolla, and G. C. Isaia, 1999, Densitometric study of developing femur: Calcified Tissue International, v. 64, p. 133-6.
Pazzaglia, U. E., G. Beluffi, A. Benetti, M. P. Bondioni, and G. Zarattini, 2011, A Review of the Actual Knowledge of the Processes Governing Growth and Development of Long Bones: Fetal and Pediatric Pathology, v. 30, p. 199-208.
Percival, C. J., and J. T. Richtsmeier, 2013, Angiogenesis and intramembranous osteogenesis: Developmental dynamics : an official publication of the American Association of Anatomists, v. 242, p. 909-22.
Piola, V., B. Posch, H. Radke, G. Telintelo, and M. E. Herrtage, 2012, Magnetic resonance imaging features of canine incomplete humeral condyle ossification: Vet Radiol Ultrasound, v. 53, p. 560-5.
Pomriaskinsky- Kobozieff, N., and N. Kobozieff, 1954, Étude radiologique de l'ossiffication du squelette du main du Chien aux divers stade de son évolution, de la naissance à l'âge adulte: Recueil de Médecine Vétérinaire, v. Tome CXXX, p. 617-646.
Retterer, E., 1884, Contribution au developpment di Squelette des extremites chezle Mammifers: Journal de l'Anatomie, v. 20, p. 467-614.
Riser, W. H., 1973, Growth and development of the normal canine pelvis, hip joints and femurs from birth to maturity: a radiographie study: Journal of the American Veterinary Radiology Society, v. 14, p. 24-34.
Riser, W. H., 1975, The dog as a model for the study of hip dysplasia Growth, form, and development of the normal and dysplastic hip joint: Veterinary pathology, v. 12, p. 229-334.
Rivas, R., and F. Shapiro, 2002, Structural stages in the development of the long bones and epiphyses: a study in the New Zealand white rabbit: The Journal of bone and joint surgery. American volume, v. 84-A, p. 85-100.
Rolfe, R., K. Roddy, and P. Murphy, 2013, Mechanical regulation of skeletal development: Current osteoporosis reports, v. 11, p. 107-16.
Ronald L. Burk, N. A., 1996, Small Animal Radiology and Ultrasonography: a diagnostic atlas and text.
Salle, B. L., P. Braillon, F. H. Glorieux, J. Brunet, E. Cavero, and P. J. Meunier, 1992, Lumbar bone mineral content measured by dual energy X-ray absorptiometry in newborns and infants: Acta Paediatr, v. 81, p. 953-8.
Schebitz, H., and H. Wilkens, 1978, Atlas of radiographic anatomy of the Dog and the Cat: Berlin , Philadelphia, Parey, VP Sauders.
Schmeling, A., G. Geserick, W. Reisinger, and A. Olze, 2007, Age estimation: Forensic science international, v. 165, p. 178-81.

Schmidt, M. J., A. C. Neumann, K. H. Amort, K. Failing, and M. Kramer, 2011, Cephalometric measurements and determination of general skull type of Cavalier King Charles Spaniels: Vet Radiol Ultrasound, v. 52, p. 436-40.
Schmidt, S., I. Nitz, S. Ribbecke, R. Schulz, H. Pfeiffer, and A. Schmeling, 2013a, Skeletal age determination of the hand: a comparison of methods: International journal of legal medicine, v. 127, p. 691-8.
Schmidt, S., M. Schiborr, H. Pfeiffer, A. Schmeling, and R. Schulz, 2013b, Age dependence of epiphyseal ossification of the distal radius in ultrasound diagnostics: International journal of legal medicine, v. 127, p. 831-8.
Scholotthaurer, C. F., 1952, The Time of Closure of the Lower Femoral Epiphysis and Upper tibial ephyphis in the Dog as determined by roentgenogram: Am J Vet Res, v. 13, p. 90.
Seoudi, K., 1948, X-ray examination of "epiphyseal union" asan aid to the estimation of age in dog: Veterinary Journal, v. 104, p. 150-5.
Shimizu, H., S. Yokoyama, and H. Asahara, 2007, Growth and differentiation of the developing limb bud from the perspective of chondrogenesis: Development, growth & differentiation, v. 49, p. 449-54.
Shum, L., C. M. Coleman, Y. Hatakeyama, and R. S. Tuan, 2003, Morphogenesis and dysmorphogenesis of the appendicular skeleton: Birth defects research. Part C, Embryo today : reviews, v. 69, p. 102-22.
Smith, R. N., 1960a, Radiological observations on the limbs of young greyhounds: J Small Anim Pract, v. 1, p. 84-90.
Smith, R. N., 1964, The pelvis of the young dog.: *Veterinary Record*, v. 76, p. 975-979.
Smith, R. N., and J. Allcock, 1960, Epiphyseal fusion in the grey-hound: Vet Rec, v. 72, p. 75-79.
Smith, R. N. a. A., J., 1960b, Epiphyseal fusion in the grey-hound: Vet Rec, v. 72, p. 75-79.
Smolders, L. A., N. Bergknut, G. C. Grinwis, R. Hagman, A. S. Lagerstedt, H. A. Hazewinkel, M. A. Tryfonidou, and B. P. Meij, 2013, Intervertebral disc degeneration in the dog. Part 2: chondrodystrophic and non-chondrodystrophic breeds: Vet J, v. 195, p. 292-9.
Sumner-Smith, G., 1966, Observations on epiphyseal fusion in the canine appendicular skeleton: J Small Anim Pract, v. 7, p. 303.
Tandon, N., C. H. Fall, C. Osmond, H. P. Sachdev, D. Prabhakaran, L. Ramakrishnan, S. K. Dey Biswas, S. Ramji, A. Khalil, T. Gera, K. S. Reddy, D. J. Barker, C. Cooper, and S. K. Bhargava, 2012, Growth from birth to adulthood and peak bone mass and density data from the New Delhi Birth Cohort: Osteoporosis international : a journal established as result of cooperation between the European Foundation for Osteoporosis and the National Osteoporosis Foundation of the USA, v. 23, p. 2447-59.
Ticer, J. W., 1984, Radiographic Technique in Veterinary Practice: Philadelphia.
Todhunter, R. J., T. A. Zachos, R. O. Gilbert, H. N. Erb, A. J. Williams, N. Burton-Wurster, and G. Lust, 1997, Onset of epiphyseal mineralization and growth plate closure in radiographically normal and dysplastic Labrador retrievers: J Am Vet Med Assoc, v. 210, p. 1458-62.
Tsukahara, H., M. Sudo, M. Umezaki, Y. Fujii, M. Kuriyama, K. Yamamoto, and Y. Ishii, 1993, Measurement of lumbar spinal bone mineral density in preterm infants by dual-energy X-ray absorptiometry: Biol Neonate, v. 64, p. 96-103.
Vanden Berg-Foels, W. S., S. J. Schwager, R. J. Todhunter, and A. P. Reeves, 2011, Femoral head shape differences during development may identify hips at risk of degeneration: Annals of Biomedical Engineering, v. 39, p. 2955-63.
Vanden Berg-Foels, W. S., R. J. Todhunter, S. J. Schwager, and A. P. Reeves, 2006, Effect of early postnatal body weight on femoral head ossification onset and hip osteoarthritis in a canine model of developmental dysplasia of the hip: Pediatr Res, v. 60, p. 549-54.
Wongdee, K., N. Krishnamra, and N. Charoenphandhu, 2012, Endochondral bone growth, bone calcium accretion, and bone mineral density: how are they related?: The journal of physiological sciences : JPS, v. 62, p. 299-307.

Wu, F. M., A. Hedhammar, and L. Krook, 1974, Overnutrition and skeletal disease. An experimental study in growing Great Dane dogs. IX. The long bones: Cornell Vet, v. 64, p. Suppl 5:83-114.
Yonamine, H., N. Ogi, T. Ishikawa, and H. Ichiki, 1980, Radiographic studies on skeletal growth of the pectoral limb of the beagle: Nihon juigaku zasshi The Japanese journal of veterinary science, v. 42, p. 417-25.
Zoetis, T., M. S. Tassinari, C. Bagi, K. Walthall, and M. E. Hurtt, 2003, Species comparison of postnatal bone growth and development: Birth Defects Res B Dev Reprod Toxicol, v. 68, p. 86-110.
Zotti, A., M. Gianesella, N. Gasparinetti, E. Zanetti, and B. Cozzi, 2011, A preliminary investigation of the relationship between the "moment of resistance" of the canine spine, and the frequency of traumatic vertebral lesions at different spinal levels: Research in Veterinary Science, v. 90, p. 179-84.
Zotti, A., M. Isola, E. Sturaro, L. Menegazzo, P. Piccinini, and D. Bernardini, 2004, Vertebral mineral density measured by dual-energy X-ray absorptiometry (DEXA) in a group of healthy Italian boxer dogs: J Vet Med A Physiol Pathol Clin Med, v. 51, p. 254-8.

Acknowledgements

Prof. Veronesi for her precious advices in veterinary neonatology.

Dr. Rota for recruitment of the sample, Dr. Meloni for sharing my study.

Dr. Bronzo for supporting statistical analysis.

Prof. Modina, Dr. Tessaro, Dr. Lodi for supporting histological analysis.

Radiology technicians for supporting x-ray room activities.